

Diverse functions of multidrug and toxin extrusion (MATE) transporters in citric acid efflux and metal homeostasis in *Medicago truncatula*

Junjie Wang^{1,†}, Qiuqiang Hou^{1,†}, Penghui Li¹, Lina Yang², Xuecheng Sun³, Vagner A. Benedito² , Jiangqi Wen⁴, Beibei Chen¹, Kirankumar S. Mysore⁴ and Jian Zhao^{1,*} 

¹National Key Laboratory of Crop Genetic Improvement, Huazhong Agricultural University, Wuhan 430075, China,

²Division of Plant & Soil Sciences, West Virginia University, Morgantown, WV 26506, USA,

³College of Resources & Environment, Huazhong Agricultural University, Wuhan 430075, China, and

⁴Plant Biology Division, the Samuel Roberts Noble Foundation, Ardmore, OK 73401, USA

Received 9 August 2016; revised 14 December 2016; accepted 19 December 2016; published online 4 January 2017.

*For correspondence (e-mail jzhao2@qq.com).

[†]These authors contributed equally to the work.

SUMMARY

The multidrug and toxin extrusion (MATE) transporter family comprises 70 members in the *Medicago truncatula* genome, and they play seemingly important, yet mostly uncharacterized, physiological functions. Here, we employed bioinformatics and molecular genetics to identify and characterize MATE transporters involved in citric acid export, Al³⁺ tolerance and Fe translocation. MtMATE69 is a citric acid transporter induced by Fe-deficiency. Overexpression of *MtMATE69* in hairy roots altered Fe homeostasis and hormone levels under Fe-deficient or Fe-oversupplied conditions. MtMATE66 is a plasma membrane citric acid transporter primarily expressed in root epidermal cells. The *mtmate66* mutant had less root growth than the wild type under Al³⁺ stress, and seedlings were chlorotic under Fe-deficient conditions. Overexpression of *MtMATE66* rendered hairy roots more tolerant to Al³⁺ toxicity. MtMATE55 is involved in seedling development and iron homeostasis, as well as hormone signaling. The *mtmate55* mutant had delayed development and chlorotic leaves in mature plants. Both knock-out and overexpression mutants of *MtMATE55* showed altered Fe accumulation and abnormal hormone levels compared with the wild type. We demonstrate that the zinc-finger transcription factor MtSTOP is essentially required for *MtMATE66* expression and plant resistance to H⁺ and Al³⁺ toxicity. The proper expression of two previously characterized MATE flavonoid transporters *MtMATE1* and *MtMATE2* also depends on several transcription factors. This study reveals not only functional diversity of MATE transporters and regulatory mechanisms in legumes against H⁺ and Al³⁺ stresses, but also casts light on their role in metal nutrition and hormone signaling under various stresses.

Keywords: citrate efflux, H⁺ and Al³⁺ toxicity, Fe translocation, MATE transporter, zinc finger, transcriptional regulation.

INTRODUCTION

Acid soil syndrome occurs in many crops in regions that account for more than 50% of arable land globally, causing huge yield losses every year around the world (Delhaize *et al.*, 2012; Kochian *et al.*, 2015). Acid soil syndrome consists of phytotoxicity as a result of excess metal ions, including aluminum (Al³⁺), manganese (Mn²⁺) and protons (H⁺), and deficiency of essential nutrients, including phosphorus, calcium and magnesium (Kobayashi and Nishizawa, 2012; Kochian *et al.*, 2015). Among these, H⁺ and Al³⁺ rhizotoxicity are the major stresses in acidic soils, causing oxidative stress, lipid composition changes,

membrane disintegrity, mitochondria dysfunction, protein denaturation, DNA damage and cell-cycle blockage (Zhao *et al.*, 2011b; Delhaize *et al.*, 2012). Multiple mechanisms have been implicated in plant response and tolerance to Al³⁺ stress. Secretion of the Al-chelating organic acids malate and citrate into the rhizosphere by plant Al-activated malate transporter (ALMT) and multidrug and toxin extrusion (MATE) transporters, respectively, is one of the primary Al³⁺ resistance mechanisms (Hoekenga *et al.*, 2006; Liu *et al.*, 2009; Liang *et al.*, 2013). The transporter-mediated root extrusion of organic acids detoxifies

rhizotoxic Al^{3+} and Cu^{2+} ions and improves the availability of phosphorus and iron (Delhaize *et al.*, 2012; Kobayashi and Nishizawa, 2012; Kochian *et al.*, 2015). In addition to transporters, several zinc-finger transcription factors, such as SENSITIVE TO PROTON RHIZOTOXICITY 1 (STOP1), STOP2, ALUMINUM RESISTANCE TRANSCRIPTION FACTOR 1 (ART1) and CALMODULIN-BINDING TRANSCRIPTION ACTIVATOR 2, have been functionally characterized in different plant species to regulate these membrane transporters in response to acidic soil and Al stress (Iuchi *et al.*, 2007; Yamaji *et al.*, 2009; Kobayashi *et al.*, 2014; Tokizawa *et al.*, 2015). Given the importance of transporters and the molecular complexity of Al and proton rhizotoxicity, the mechanisms by which these transporters function and their regulation are not fully understood (Liu *et al.*, 2009). In addition to H^+ and Al^{3+} rhizotoxicity observed under acidic soil conditions, excess essential trace elements in acidic soils, such as iron and zinc, also trigger phytotoxicity (Kobayashi and Nishizawa, 2012). These cations form complex interactions with diverse molecules in the cell, and are centrally involved in many physiological and stress conditions (Pineau *et al.*, 2012). Understanding transporter-mediated uptake, transport and distribution of these metal ions will shed light on plant response and tolerance to acidic soils and heavy metal stress.

The MATE transporter family is part of the multidrug resistance transporter superfamily, based on their phylogenetic relationships, overall protein structure and number of transmembrane domains (<http://www.tcdb.org>; Ren and Paulsen, 2005). MATEs are secondary transporters that mediate chemical efflux by coupling with electrochemical gradients (H^+ or Na^+) across the membrane (Saier and Paulsen, 2001; Moriyama *et al.*, 2008). Since the first MATE transporters from bacteria were characterized (Morita *et al.*, 1998; Brown *et al.*, 1999), many MATE genes from prokaryotes and eukaryotes, including plants, have been isolated and characterized (Omote *et al.*, 2006; Kuroda and Tsuchiya, 2009; Takanashi *et al.*, 2013). In contrast to mammalian genomes, which only have a few MATE genes, plant genomes often encode a vast number of membrane transporters. For example, the Arabidopsis genome contains at least 54 MATE genes, *Oryza sativa* (rice) has 40 MATE genes and larger crop genomes contain even more MATE transporters, e.g. *Glycine max* (soybean) has 117 MATE genes (Liu *et al.*, 2016), but far fewer than 40 plant MATEs have been functionally characterized. These plant MATE transporters are involved in diverse physiological and metabolic processes in plant growth and development (Burko *et al.*, 2011): nutrient homeostasis (Green and Rogers, 2004; Liu *et al.*, 2009); transport of hormones such as abscisic acid (ABA), salicylic acid (SA) and auxin (Serrano *et al.*, 2013; Yamasaki *et al.*, 2013; Zhang *et al.*, 2014); primary and secondary metabolisms (Yazaki, 2005; Zhao

and Dixon, 2009; Dobritsch *et al.*, 2016); and stress responses (Yamasaki *et al.*, 2013).

Legume crops, such as soybean and *Medicago sativa* (alfalfa), are sensitive to acidic soils and Al^{3+} stresses, which severely restrict legume growth and yield (Liu *et al.*, 2016). Limited information is available for legume response and tolerance to low pH and Al stresses, however, largely because of their complex genetics, large genomes and intricate resistance mechanisms (Chandran *et al.*, 2008; Liu *et al.*, 2016). As a model legume, *Medicago truncatula* (barrel medic) has been well developed for representative genetic studies on legumes. This species has rich molecular and genetic resources (Benedito *et al.*, 2008; Zhao and Dixon, 2009; Young *et al.*, 2011), in particular a large publicly available *M. truncatula* mutant collection (Tadege *et al.*, 2008). Given the importance and diverse functions of plant MATE transporters in response to various stresses, including H^+ and Al^{3+} phytotoxicity, in this study we performed an in-depth dissection of *M. truncatula* MATE transporters involved in Al tolerance and Fe nutrition. Through characterization of *M. truncatula* mutants for these MATE transporters and their regulators, we show that the MtMATE transporters are not only involved in response to Al^{3+} stresses and Fe nutrition indirectly, but are also directly involved in flavonoid transport. Transcription of these MATEs is tightly regulated by transcription factors, including MtSTOP, which is characterized here as a C_2H_2 zinc-finger factor regulating the *Medicago* response to H^+ and Al^{3+} phytotoxicity. This study provides insight into the physiological roles of citric acid efflux MATE transporters in the legume plant, thus paving a road towards improving legume tolerance to acidic soils and Al^{3+} stress.

RESULTS

The MATE family in *M. truncatula* consists of a large number of transporters

The *M. truncatula* genome sequence version 4.0 (<http://phytozome.jgi.doe.gov/pz/>) contains 74 predicted genes coding for MATE proteins (Appendix S1). Of these, four predicted MATE genes code for very short peptides, and so are possibly pseudogenes, whereas others also have alternative splice forms (Appendices S1, S2). A phylogenetic tree was generated using all 70 full-length *M. truncatula* MATE proteins, named according to the clustering, following two previously characterized MATE proteins, MtMATE1 and MtMATE2. The MtMATEs can be grouped into four distinct clades (Figure 1a; Zhao and Dixon, 2009; Zhao *et al.*, 2011a). Interestingly, a fifth clade appears when a comprehensive phylogenetic tree containing *M. truncatula*, Arabidopsis, other functionally characterized MATE transporters, and MATEs from prokaryotes and animal species was created to compare the evolution of *M. truncatula* MATEs (Figure 1b). This suggests that MATEs from

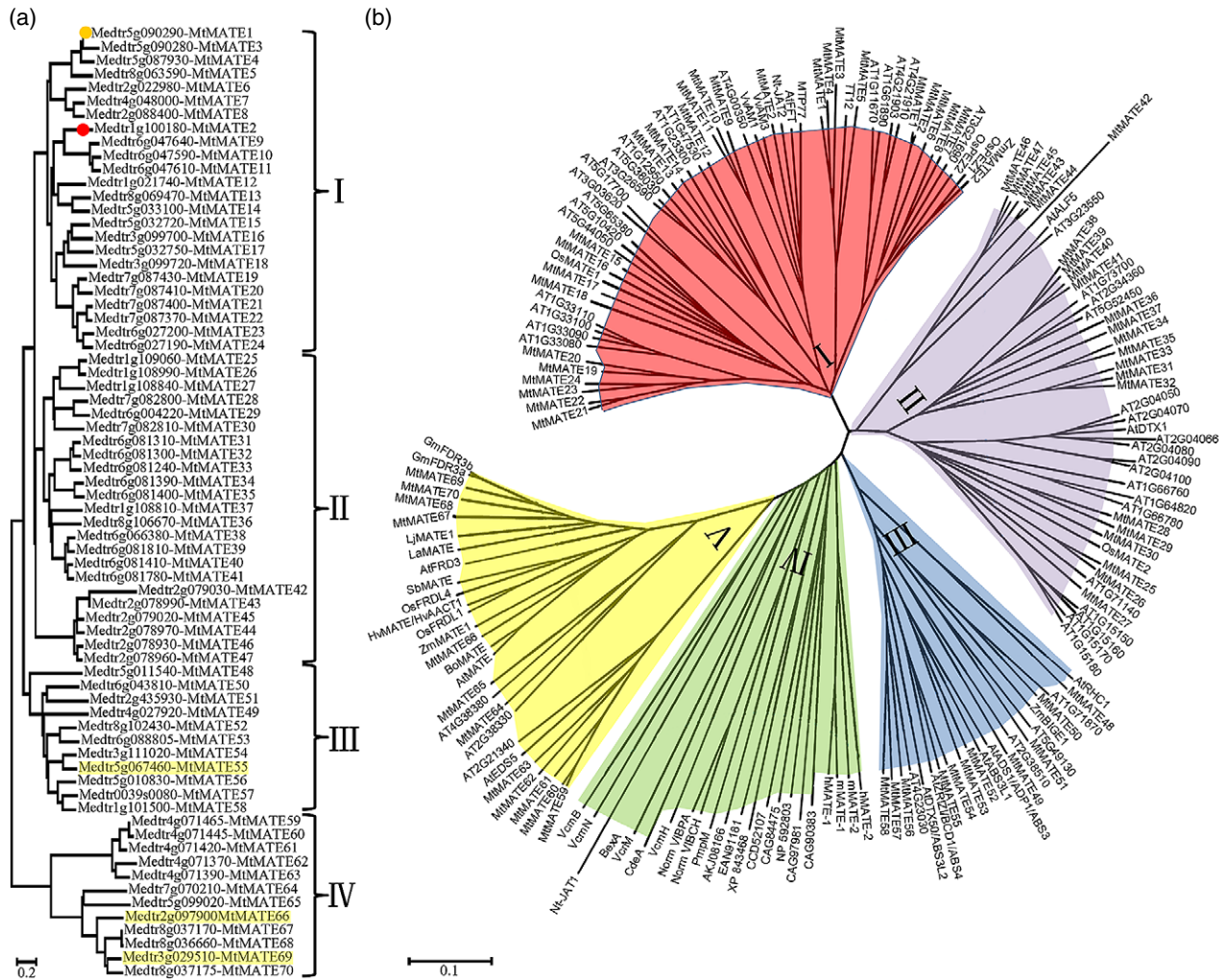


Figure 1. Phylogenetic analysis of MATE transporters in the *Medicago truncatula* genome. (a) Phylogenetic tree and nomination of all *M. truncatula* MATE transporters (70 MATEs in total). MtMATE1 and MtMATE2 reported previously are highlighted with colored circles. MtMATE55, MtMATE66 and MtMATE69, highlighted in yellow, are studied here. (b) Phylogenetic analysis of *M. truncatula* MATE transporters, together with *Arabidopsis thaliana* MATEs and functionally characterized MATEs from other species and non-plant MATEs. The phylogenetic tree was generated with protein sequences by the maximum-likelihood method, with 1000 bootstraps based on JTT matrix-based model in MEGA 6.0. The tree is drawn to scale, with branch lengths measured in number of substitutions per site. The distinct clades are assigned according groups.

prokaryotes and animal species evolved independently from the MATEs of plants. Tandem duplication and syntenic paralog analysis of *Medicago* and *Arabidopsis* MATEs revealed evolutionary conservation, likely in both structure and function (Figure S1; Tables S1, S2). We analyzed MATE transporters involved in the secretion of organic acids or compounds that facilitate Fe uptake or translocation, and the chelation of metal ions.

MATEs in clade I include several characterized transporters that transport flavonoids, alkaloids and other phenolics (Yazaki, 2005; Zhao *et al.*, 2011a; Zhao, 2015). Among them, rice phenolic exporters PHENOLICS EFFLUX ZERO 1 and 2 (PEZ1 and PEZ2) are involved in Fe solubilization and uptake (Bashir *et al.*, 2011; Ishimaru *et al.*, 2011). On the other hand, MATEs in clade II are mostly

uncharacterized, except for ALF5 and DTX1 (Diener *et al.*, 2001; Li *et al.*, 2002). Clade III encompasses a group of recently characterized transporters involved in plant development and growth. These include BCD1, which localizes to Golgi bodies and has a role in Fe nutrition and organ initiation and development, affecting hypocotyl cell elongation under light (Burko *et al.*, 2011; Seo *et al.*, 2012), and Medtr5g067460.1 (MtMATE55), which is also expressed in flowers, hypocotyls and vegetative buds (Figures 1, S2). Clade III also includes AtDTX50, a plasma membrane ABA efflux transporter (Zhang *et al.*, 2014), Arabidopsis RESISTANT TO HIGH CO₂ 1 (RHC1; Tian *et al.*, 2015), ALTERED DEVELOPMENT PROGRAM 1 (ADP1; Li *et al.*, 2015b) and the maize *trans*-Golgi membrane-localized BIG EMBRYO 1 (ZmBIGE1; Suzuki *et al.*, 2015). These MATE transporters

directly or indirectly participate in the translocation of plant hormones or signaling molecules from the sites of synthesis to the target sites, and thereby regulate plant development and growth. Although MATEs from prokaryotes and other eukaryotic organisms are included in clade IV, the rest of the MATEs form a unique clade, clade V. Clade V contains citric acid exporters that secrete organic acids to the apoplast in order to either chelate Al^{3+} in the rhizosphere, being involved in alleviating Al^{3+} toxicity in acidic soils, or facilitate Fe^{2+} or Zn^{2+} translocation from roots to shoots by secreting citric acid into the vascular system, and forming a transportable citric acid–Fe complex. Al-tolerance MATEs include MtMATE66 (Medtr2g097900.1), OsFRDL1, AtMATE and SbMATE (Magalhaes *et al.*, 2007; Durrett *et al.*, 2007; Liu *et al.*, 2009; Yokosho *et al.*, 2009; Figure 1b), Fe^{2+} - or Zn^{2+} -translocation MATEs include FER-ERIC REDUCTASE DEFECTIVE 3 (FRD3) from Arabidopsis, GmFRD3a and GmFRD3b from soybean, MtMATE69 (Medtr3 g029510.1), and LjMATE1, a citric acid transporter (Green and Rogers, 2004; Takanashi *et al.*, 2013; Figure 1b). Clade V also contains Arabidopsis ENHANCED DISEASE SUSCEPTIBILITY 5, which is localized to the chloroplast envelope and transports SA out of the organelle for triggering the systemic acquired resistance (Yamasaki *et al.*, 2013).

Diverse expression patterns of MATE transporter genes in *Medicago truncatula*

We retrieved gene expression data from MGEA (<http://mtgea.noble.org/v3/>) with *M. truncatula* Affymetrix array probe sets Mtr.21348.1.S1_at for MtMATE55, Mtr.23405.1.S1_at and Mtr.35696.1.S1_at for MtMATE66, and Mtr.8402.1.S1_at, Mtr.15345.1.S1_at and Mtr.41827.1.S1_at for MtMATE69, and probe sets for other MATEs on chip (Figures S3, S4). This study revealed that members of the MATE family are expressed in all organs of the *M. truncatula* plant, from the root tip to both flower and seed (Figure S3). Expression of most MATE genes responded to hormone application, salt stress, drought, heat, yeast elicitor, methyl jasmonate, pathogens and insect attack (Figure S3a–c). The tissue expression pattern may reflect the indispensable functions that MATEs play in a wide range of cellular processes (Figure S5). RNA-Seq and quantitative real-time PCR (qRT-PCR) analyses showed that each of these genes presents a distinct transcriptional profile in the mature plant. MtMATE55 is mostly expressed in hypocotyls, vegetative buds and leaves (Figure S2). MtMATE66 is primarily expressed in leaves, stems and nodules, and at low levels in vascular tissues of roots, stems and pods (Figures S4, S5). MtMATE69 shows partially complementary expression patterns to MtMATE66, with strong and primary expression in roots and stems (Figure S4). Further dissection of the whole plant indicated that, compared with the expression levels

in young roots and stems, both MtMATE69 and MtMATE66 were highly expressed in main stems and roots, where vascular tissues predominate. Both of them were also expressed in root elongation zones and tips, where the uptake of nutrients usually takes place (Figure S6). The data suggest that MtMATE66 and MtMATE69 are both highly induced in plants upon salinity and drought stress (Figures S4–S6). NaCl and drought stresses also induced MtMATE55 expression (Figures S4–S6). The expression profiles of MtMATE genes in the databases, including the *Tnt1* insertion mutants to the transcription factors *mtpar*, *mtnst1*, *mtwd40-1*, *mttt8* and *mtccr*, showed that many MATE genes are differentially regulated in these mutants, indicating that their transcription might be regulated by these transcription factors (Figures S3, S4).

Identification and generation of MtMATE and MtSTOP knock-out and overexpression mutants

Although no mutant for MtMATE69 was available in the *Tnt1* insertion mutant collection, two knock-out lines for MtMATE55 (NF5006 and NF11176) were identified by reverse screening. Full-length MtMATE66 transcript was not detected in the corresponding homozygous *mtmate66-2* line (NF11176), and only a trace level was found in the homozygous *mtmate66-1* line (NF5006), perhaps because of the proximity of the *Tnt1* insertion site to the 3' end of the transcribed region (Figure 2a, b). Screening of the NF0245 line resulted in the isolation of a homozygous knock-out mutant, *mtmate55-1*. MtMATE55 transcripts were not detected in the *mtmate55-1* mutant, whereas clear, full-length transcripts were detected in the R108 wild type (Figure 2a, b).

To explore the mechanism of MATE transporter regulation in response to H^+ and Al^{3+} stresses, we identified MtSTOP (Medtr3g087120.1), an Arabidopsis AtSTOP1 homolog from *M. truncatula*. Two MtSTOP mutants were identified in the *Tnt1* collection. MtSTOP transcripts were not detected in the homozygous *mtstop-2* line (NF7142), whereas less than 30% of the transcript remained in *mtstop-1* (NF5453) (Figure 2a, b). MtSTOP, represented by probe sets Mtr.35842.1.S1_at and Mtr.13291.1.S1_at, showed higher expression in root than in other tissues (Figure S7). In order to characterize the functions of MtMATE69, MtMATE55 and MtMATE66, as well as those of MtSTOP, we created transgenic hairy roots overexpressing these MtMATE and MtSTOP genes (Figure 2c).

Phenotypes of *Medicago* MATE transporter and MtSTOP mutants

Under normal conditions, the growth of *mtmate66-1*, *mtmate66-2*, *mtstop-1* and *mtstop-2* homozygous mutant lines was comparable with that of wild-type R108; however, the *mtmate55-1* mutant showed retarded growth,

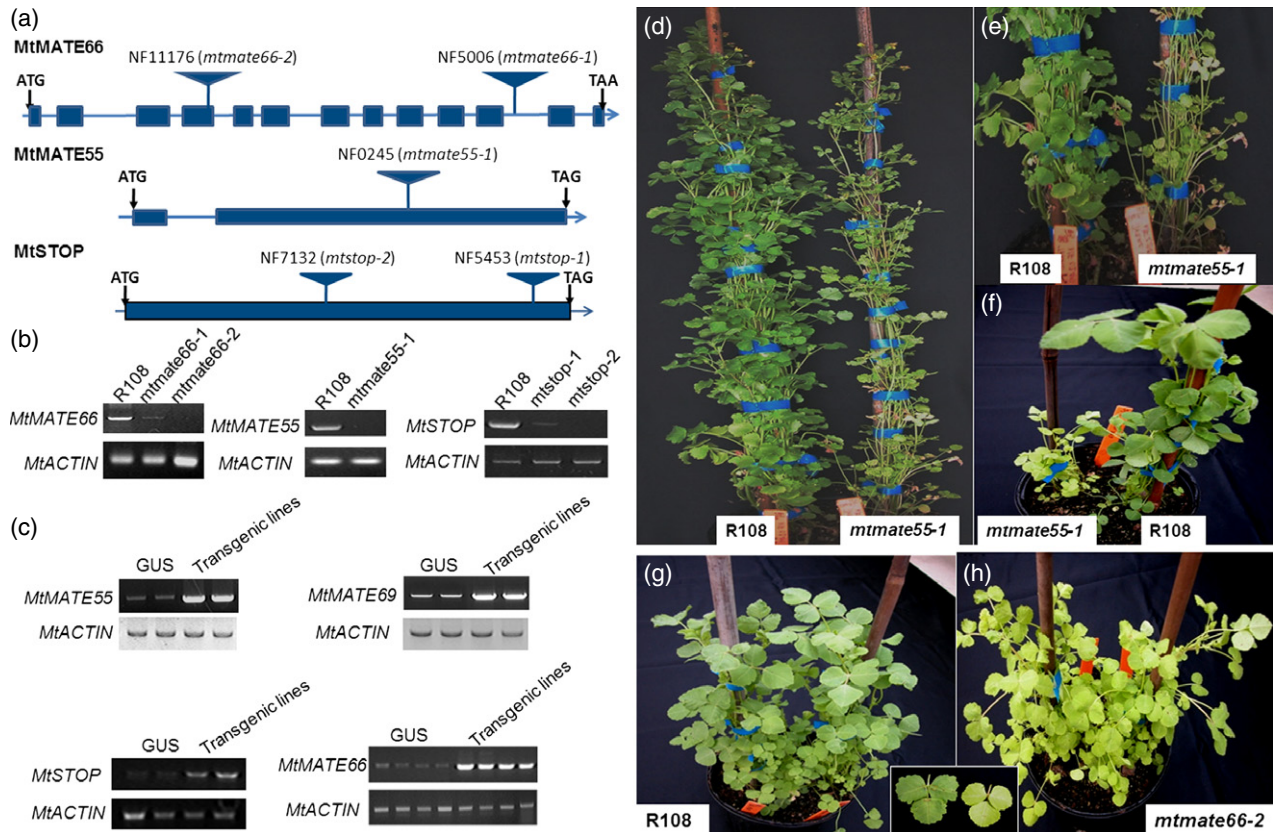


Figure 2. Characterization of *Tnt1* knock-out mutants and overexpression hairy root lines for *MtMATE55*, *MtMATE66*, *MtMATE69* and *MtSTOP*. (a) Positions of *Tnt1* lines with insertions in *MtMATE* and *MtSTOP* genes. Boxes indicate exons, and lines indicate introns. (b) *MtMATE* and *MtSTOP* transcripts in seedlings of the wild-type ecotype R108, *mtmate55-1* (NF0245), *mtmate66-1* (NF5006), *mtmate66-2* (NF11176), *mtstop-1* (NF5453) and *mtstop-2* (NF7132) mutants by semiquantitative RT-PCR. (c) Semi-quantitative RT-PCR analysis of transgenic hairy root lines overexpressing *MtMATE55*, *MtMATE66*, *MtMATE69* or *MtSTOP*. *MtACTIN* (*Medtr3 g095530*) was used as a housekeeping control gene for normalization. (d) The *mtmate55-1* mutants are less branched, smaller thinner plants, with chlorosis. Nine-week-old plants are shown. (e) Enlarged photos of the *mtmate55-1* mutant and the wild type (R108). More chlorosis was observed in the mutant in comparison with the wild-type R108. (f) The *mtmate55-1* mutant growing under Fe-deficiency conditions. Three-week-old *mtmate55-1* mutant shows more chlorosis and dwarfism compared with the wild-type R108 under Fe-deficient conditions. Fertilization medium was supplemented with 300 μM ferrozine instead of iron sulfate. (g, h) Comparison of 6-week-old wild-type and *mtmate66-2* plants under Fe-deficiency conditions. Like the *mtmate55-1* mutant, *mtmate66-2* also shows more drastic Fe-deficiency symptoms than the wild type under low Fe conditions.

dwarfism and chlorotic leaves (Figure 2d). The mutant plants displayed a roughly 10-day delay in the development of the first trifoliolate, in comparison with the segregant control (i.e. sibling plants from the same insertion line without the insertion in the gene under study). Mutant plants were thinner, less branched and had fewer leaves than the segregant control (Figure 2d). More chlorosis occurred in older leaves, suggesting that the leaves underwent early senescence. The height of *mtmate55-1* was approximately 80% of that of the wild-type control (Figure 2d), and the chlorophyll content in *mtmate55-1* was only 74% of the control (Figure 2e).

Under Fe-deficient conditions, the development of *mtmate55-1* plants became severely retarded, with stronger dwarfism and more chlorosis (Figure 2f). Chlorophyll content in *mtmate55-1* was only 45% of that of the control (Figure 3a). Although *mtmate66-2* plants became chlorotic, the growth rate was not significantly affected over the

3-week period of treatment, whereas *mtmate66-1* did not show perceptible differences in comparison to the control during this period (Figure 2g, h).

The altered expression of *MtMATE* and *MtSTOP* genes was detected under Fe²⁺ oversupply or deficiency, as well as with Al³⁺ exposure (Figure 3). When sufficient Fe²⁺ was supplied, only *MtMATE55* was induced (Figure 3b), whereas under Fe²⁺ deficiency, the expression of both *MtMATE66* and *MtMATE69* increased compared with the control (Figure 3c). ICP-MS revealed that although the Fe content in *mtstop* seedlings did not differ from the wild type under Fe-deficient conditions, the seedlings of both *mtmate66-2* and *mtmate55-1* mutants had altered Fe accumulation in roots and shoots, compared with the control. In particular, consistent with the chlorotic leaf phenotype, *mtmate55-1* mutant shoots showed reduced Fe content not only under Fe deficiency but also under Fe-sufficient conditions. Conversely, *mtmate55-1* roots had higher Fe levels

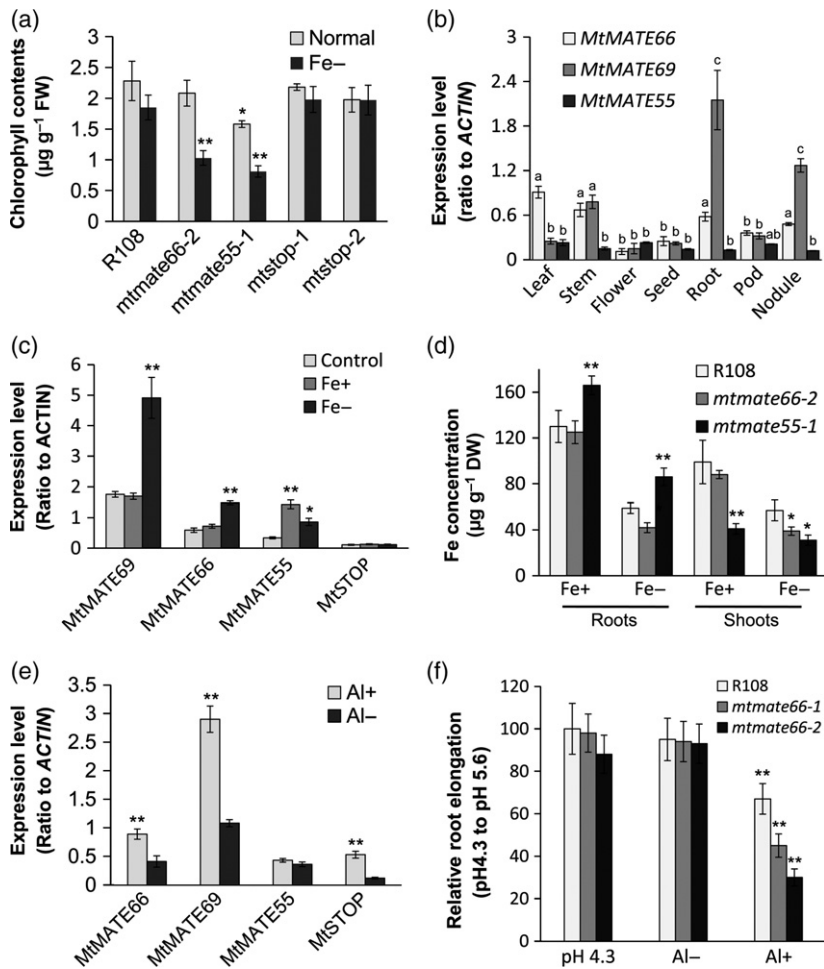


Figure 3. Characterization of *mtmate* and *mtstop* mutants under stress conditions. (a) Chlorophyll contents in leaves of *Tnt1* insertion mutants for *MtSTOP*, *MtMATE55*, *MtMATE66* under normal and Fe-deficient stressed conditions. (b) Tissue-specific expression of *MtMATE* genes. Different letters indicated the values with significant differences ($P < 0.05$) from each other. (c) Altered expression of *MtMATEs* and *MtSTOP* under Fe-deficient (Fe⁻) and Fe-oversupplied (Fe⁺) conditions. *MtACTIN* was used as a control. (d) Fe accumulation in shoots (leaves and stems) and roots of *mtmate55-1*, *mtmate66-2* under Fe-deficient (Fe⁻) and Fe-oversupplied (Fe⁺) conditions. (e) Altered expression of *MtMATEs* and *MtSTOP* under pH 4.3 with Al³⁺ (Al⁺) or without Al³⁺ (Al⁻) stress. *MtACTIN* was used as a control. (f) Root growth of *mtmate66-1* and *mtmate66-2* under different pH values (5.6 and 4.3) with (Al⁺) or without (Al⁻) a supplement of 50 μM Al³⁺. Data are represented as means \pm SDs. Differences between paired data from wild-type *R108* and each mutant plants under normal (Al⁻ or Fe⁺) or treatment (Al⁺ or Fe⁻) conditions were analyzed by Student's *t*-test ($n = 3$): * $P < 0.05$; ** $P < 0.01$.

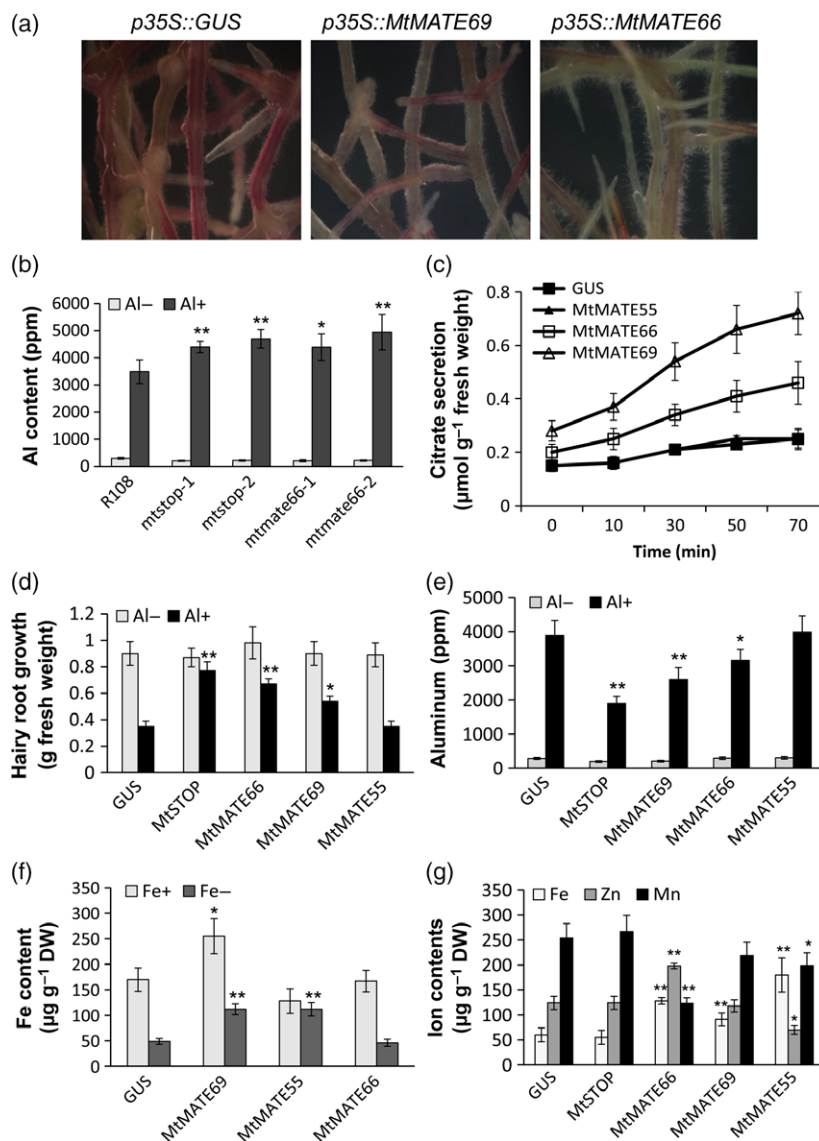
than the wild type (Figure 3d). When Fe was oversupplied, only *mtmate55-1* showed reduced Fe content in shoots (approximately 50% reduction), whereas Fe increased in roots compared with segregant controls and *mtmate66* mutants. With Al³⁺ exposure, both *MtMATE66* and *MtMATE69* and *MtSTOP* were upregulated in wild-type plants, whereas transcripts of *MtMATE55* did not change significantly (Figure 3e). Under Al³⁺ stress conditions, both *mtmate66* mutants exhibited significantly shorter roots compared with mutant plants grown on medium with no Al³⁺, suggesting that *MtMATE66* is involved in the Al³⁺ stress response (Figure 3f).

***MtMATE66*, *MtMATE69* and *MtSTOP* are involved in citric acid extrusion**

MtMATE transgenic roots did not have altered morphology compared with the control under normal conditions, but they were different under Al³⁺ stress conditions: *MtMATE66* and *MtMATE69* hairy roots grew healthier than the *GUS* hairy roots (Figure 4a). Similarly, the wild-type roots contained significantly lower levels of Al than the roots of the *MtSTOP* and *MtMATE66* insertion mutant lines

(Figure 4b). The culture medium used for growing hairy roots expressing *MtMATE66* or *MtMATE69* contained more citric acid than media with the *GUS* hairy root control (Figure 4c). Time-course monitoring of citric acid secretion into the medium showed that hairy roots expressing *MtMATE66* had the highest citric acid secretion rate. *MtMATE69* transgenic hairy roots also secreted significantly more citric acid than the *MtMATE55* or *GUS* transgenic hairy root control (Figure 4c). Without Al³⁺ stress, the *MATE* overexpressing root lines grew at similar rates; however, under Al³⁺ stress conditions, hairy root lines overexpressing *MtSTOP*, *MtMATE66* and *MtMATE69* accumulated significantly more biomass than the *GUS* control (Figure 4d). The level of Al in *MtSTOP*, *MtMATE66* and *MtMATE69* hairy root lines grown in Al³⁺-stress medium were significantly lower than those of the *GUS* control (Figure 4e). In contrast, *MtMATE55* hairy roots showed no difference in comparison with the *GUS* control under Al³⁺ stress (Figure 4d, e). These data unambiguously indicate that both *MtMATE66* and *MtMATE69* might be involved in Al³⁺ tolerance mechanisms, by facilitating citric acid secretion; however, under Fe-deficient conditions, *mtmate66-1*

Figure 4. Characterization of mutant roots and hairy root lines overexpressing *MtMATE55*, *MtMATE66*, *MtMATE69* or *MtSTOP*. (a) Transgenic hairy roots overexpressing *GUS*, *MtMATE66* and *MtMATE69*, driven by 35S promoter control grown in Al-stress medium. (b) Al accumulation in the roots of *mtstop* and *mtmate66* mutants after Al-stress (Al⁺) or non-stress (Al⁻) treatment. Contents were based on root dry weights. (c) Secretion of citric acid by hairy roots overexpressing *MtMATE55*, *MtMATE66*, *MtMATE69* or *GUS* (as a control). (d) Hairy root growth (counted as fresh weight increase) in Al stress (Al⁺) and non-Al stress (Al⁻) medium. (e) Al accumulation in the hairy roots expressing *MtMATEs* upon Al-stress (Al⁺) or non-stress (Al⁻) treatment. Contents were based on root dry weights. (f) Fe contents in hairy roots expressing *MtMATEs* grown in Fe-deficient (Fe⁻) and Fe-oversupplied (Fe⁺) medium. (g) Fe, Mn and Zn contents in hairy roots expressing *MtMATEs* and *MtSTOP* under Al-stressed conditions. Data are represented as means \pm SDs. Differences between paired data from wild-type R108 and each mutant plants or from *GUS* control and *MtMATE* or *MtSTOP* overexpression lines under normal (Al⁻ or Fe⁺) or treatment (Al⁺ or Fe⁻) conditions were analyzed by using Student's *t*-test ($n = 3$): * $P < 0.05$; ** $P < 0.01$.



and *mtmate66-2* showed reduced Fe content in roots and shoots, suggesting that *MtMATE66* may also be involved in Fe uptake or translocation (Figure 4d).

***MtMATEs* are involved in cellular Fe homeostasis and nutrition**

As *MtMATE55* transcript was induced under both Fe-deficient and -oversupplied conditions, and the *mtmate55-1* mutant displayed altered Fe accumulation, *MtMATE55* may be involved in Fe homeostasis. When *MtMATE55* was overexpressed in hairy roots, citric acid secretion was comparable with that of the wild type (Figure 4c); however, the *MtMATE55* hairy roots accumulated only approximately 50% of the Fe, compared with the *GUS* control under Fe-sufficient conditions, but contained more Fe than the control under Fe deficiency (Figure 4f).

Therefore, *MtMATE55* is indeed involved in Fe homeostasis, but apparently not in transport of citric acid or Fe. We further investigated *MtMATE69* involvement in Fe nutrition, as its expression was induced by Fe deficiency. When hairy roots overexpressing *MtMATE69* or *GUS* were grown at 10 μM Fe or 0.2 μM Fe, *MtMATE69* hairy roots accumulated significantly more Fe than the *GUS* control, whereas the Fe content of *MtMATE66* hairy roots was similar to the control under both Fe conditions (Figure 4f). As suggested by the unbalanced accumulation of metals in the *frd3* mutant (Yi and Guerinot, 1996), coordination between homeostasis of metals, such as Fe, Mn and Zn, is essential for plant tolerance to stresses (Pineau *et al.*, 2012). Further analysis of metal contents in Al³⁺-stressed *MtMATE* transgenic hairy roots suggested that *MtMATE55* and *MtMATE66* overexpression affected

the accumulation of all of three metals, whereas only Fe accumulation was affected in hairy roots overexpressing *MtMATE69* (Figure 4g).

To understand how these MtMATEs affect Fe homeostasis, we assessed Medicago *Fe³⁺ Reduction Oxidase (MtFRO)* and *IRON-REGULATED TRANSPORTER 1 (MtIRT1)* gene expression and *Fe³⁺-chelate reductase* activity in *mtmate* mutants and overexpressing hairy roots. The *M. truncatula IRT1* ortholog *MtIRT1* was also induced by Fe deficiency, suggesting that *MtIRT1* may also play a role in iron uptake from the soil (Figure 5; Vert *et al.*, 2002). As citric acid secretion was reduced in the *mtmate66* mutants, we also observed that the transcription of *MtFRO1* and *MtFRO2*, as well as the *MtIRT1* genes, were reduced further, compared with wild-type roots (Figures 5a, S8); however, transcripts of both *MtIRT1* and two *MtFRO* genes increased more in hairy roots overexpressing *MtMATE66* and *MtMATE69* than in the *GUS* control under Fe deficiency. *MtIRT1* transcripts were also higher in the *MtMATE69* line than in the *GUS* control. *MtIRT1* was reduced only in hairy roots overexpressing *MtMATE55* (Figure 5b). We tested whether MtMATEs affect root *Fe³⁺* reduction capacity, which is usually critical for Fe uptake by *MtIRT1*. Root FRO activity was decreased in *mtmate66* but not in *mtmate55*; however, increases in *Fe³⁺* reduction activity were observed in both *MtMATE66* and *MtMATE69* overexpressing hairy roots, whereas no significant change was observed in *MtMATE55* transgenic hairy roots (Figure 5c).

Altered *MtMATE* expression leads to changes in hormone levels under metal stresses

As differential growth was observed in *MATE* mutants in relation to the wild-type control, we examined whether plant hormone levels changed. We measured hormone contents in knock-out mutants and overexpressing hairy root lines under *Al³⁺* stress and *Fe²⁺* deficiency. In *mtmate55* and *mtmate66* mutants, seedlings had a yellowish color and stunted growth under Fe deficiency, higher levels of ABA and SA, and decreased levels of IAA and JA (Figure 5d). On the other hand, *mtmate66* knock-out mutants had reduced root elongation under *Al³⁺* stress and lower IAA and JA levels in the root compared with the wild-type control (Figure 5d). Interestingly, *mtmate55* mutant seedlings also had significantly higher ABA, slightly lower IAA, and similar JA and SA levels compared with the wild type under the same conditions, even though *mtmate55* did not show the root elongation phenotype. In overexpression lines of the three *MATE* genes under study, IAA and JA levels were significantly higher, whereas ABA and SA levels were lower than measured in the *GUS* control under *Al³⁺* stress (Figure 5e). Under Fe-deficiency conditions, the levels of IAA and JA were higher in *MtMATE66* and *MtMATE69* hairy roots, but not significantly different in *MtMATE55*, although ABA levels were lower in all three

MtMATE transgenic hairy roots compared with the *GUS* hairy roots (Figure 5e).

Complementation of *mtmate55* and *mtmate66* mutants, and verification of phenotypes

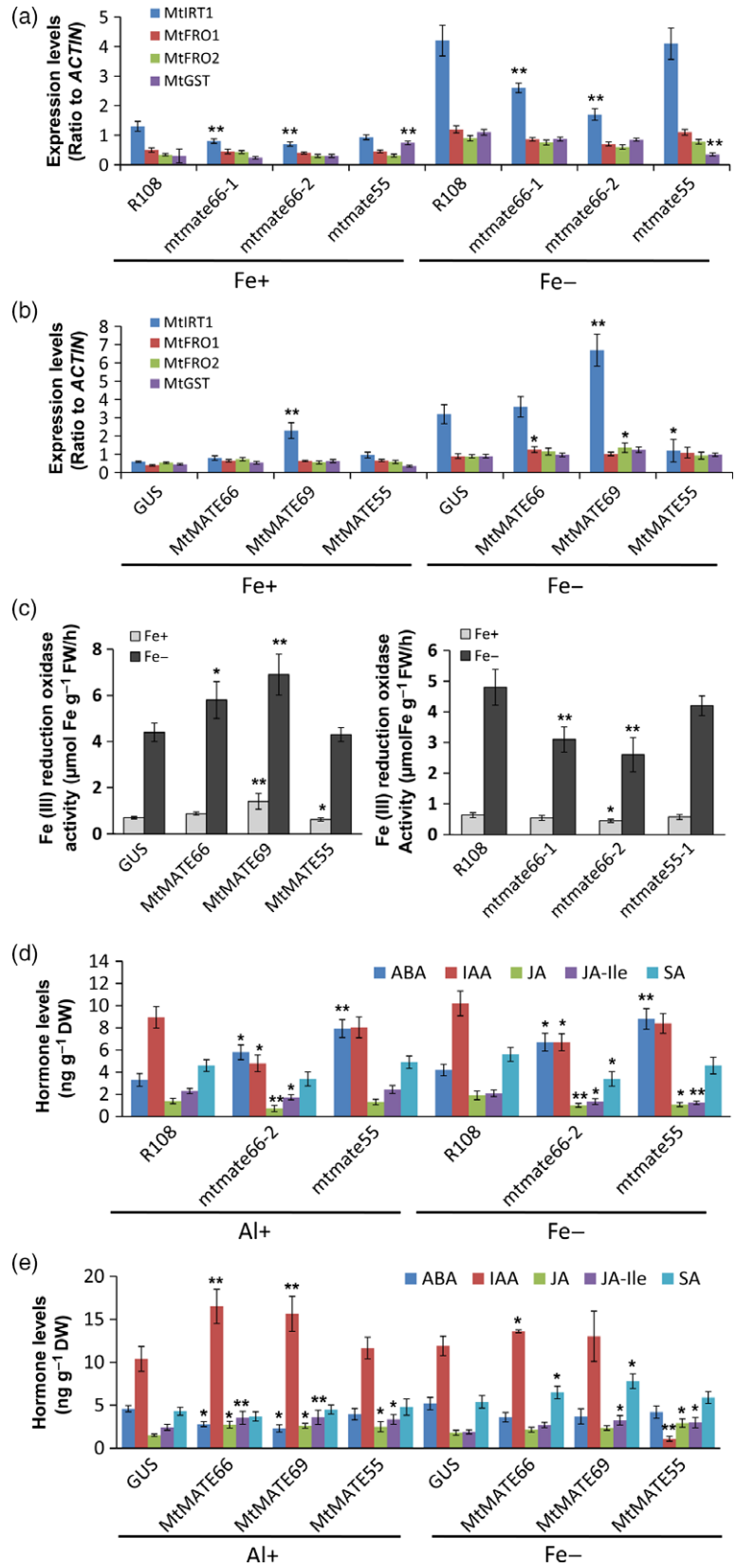
To confirm whether the *mtmate55* and *mtmate66* phenotypes result from the loss of their respective gene functions, we conducted segregation analyses on these mutants for three generations. In two independent *mtmate66* mutant lines, we observed that *Al³⁺* sensitivity was always associated with *Tnt1* insertions in *MtMATE66*, with *mtmate66-2* consistently showing more severe phenotypes than *mtmate66-1*. An analysis of all recovered sequences flanking *Tnt1* insertion sites within the genome of each of these lines also suggests that these insertions are not affecting metal transporter genes (Tables S3–S7). Overexpression of *MtMATE66* in hairy roots of *mtmate66-2* completely restored citric acid secretion to the levels of the wild-type hairy root control under *Al³⁺* stress (Figure 6a, b). Altogether, these data demonstrate that ablation of *MtMATE66* is responsible for the phenotypes observed in the *mtmate66* mutants.

The altered morphological phenotypes, including dwarfism, delayed development and higher Fe accumulation in the *mtmate55-1* mutant (NF0245) under Fe deficiency, were clearly associated with the knock-out of the *MtMATE55* gene. Although the *mtmate55-1* line has several insertions in glycosyltransferase genes, which may be related to lignin or cell wall biosynthesis that could cause dwarfism, the detection of cell wall and lignin structures by autofluorescence microscopy revealed normal-appearing cell wall and lignin (Figures S3, S9). Genetic complementation of the *MtMATE55* mutant also restored Fe accumulation under Fe-deficiency (Figure 6c), indicating that the mutant phenotypes reported here were related to the loss of *MtMATE55* function.

MtSTOP is a C2H2 zinc-finger transcription factor regulating sensitivity to *H⁺* and *Al³⁺* stresses

Phylogenetic analysis showed that *MtSTOP* is closest to *AtSTOP2* and other soybean homologs (Figure 7a). *MtSTOP* is expressed in roots, stems, nodules and other tissues (Figure S7). *MtSTOP* is upregulated by acidic pH and *Al³⁺* stress, or by a combination of the two (Figure 7b). Under normal conditions, *mtstop* mutants did not display altered growth or morphology; however, both mutant seedlings were sensitive to low pH (pH 4.3) and *Al³⁺* stress, as indicated by drastically reduced root elongation (Figure 7c). More *Al* was accumulated in the mutant roots compared with the segregation control, and root-secreted citric acid in the mutant roots was significantly lower in both normal and *Al* stress conditions (Figure 7d, e). Correspondingly, *MtSTOP* hairy roots secreted more citric and malic acid, and the time course study indicated that the

Figure 5. Fe reduction and uptake by *Medicago truncatula* MATE mutant roots. *Medicago mtmate66-2* and *mtmate55-1* mutants (4 weeks old) were treated under Fe-deficiency and Fe-oversupplied conditions, as described in the Experimental procedures section. Roots were used for testing gene expression and Fe(III) reduction oxidase activity assay. (a) Expression of *MtFROs* and *MtIRT1* in R108 wild-type, *mtmate66s* and *mtmate55-1* roots under Fe-deficiency and Fe-sufficient conditions. (b) Expression of *MtFROs* and *MtIRT1* in the hairy roots from R108 wild-type plants overexpressing *GUS*, *MtMATE55*, *MtMATE69*, or *MtMATE66* under Fe-deficiency and Fe-sufficient conditions. (c) Fe(III) reduction oxidase activity in roots derived from R108, *mtmate66* mutants and *mtmate55-1* plants, or R108 hairy roots overexpressing *GUS*, *MtMATE55*, *MtMATE66* or *MtMATE69* under Fe-deficiency and Fe-sufficient conditions. (d) Hormone changes in *mtmate* knock-out mutants under Al stress and Fe-deficiency conditions. (e) Hormone changes in *MtMATE* expressing hairy roots under Al stress and Fe-deficiency conditions. Data are represented as means \pm SDs. Differences between paired data from wild-type R108 and *mtmate* mutants or from *GUS* control and *MtMATE* overexpression lines under normal (Al⁻ or Fe⁺) or treatment (Al⁺ or Fe⁻) conditions were analyzed by Student's *t*-test ($n = 3$): * $P < 0.05$; ** $P < 0.01$.



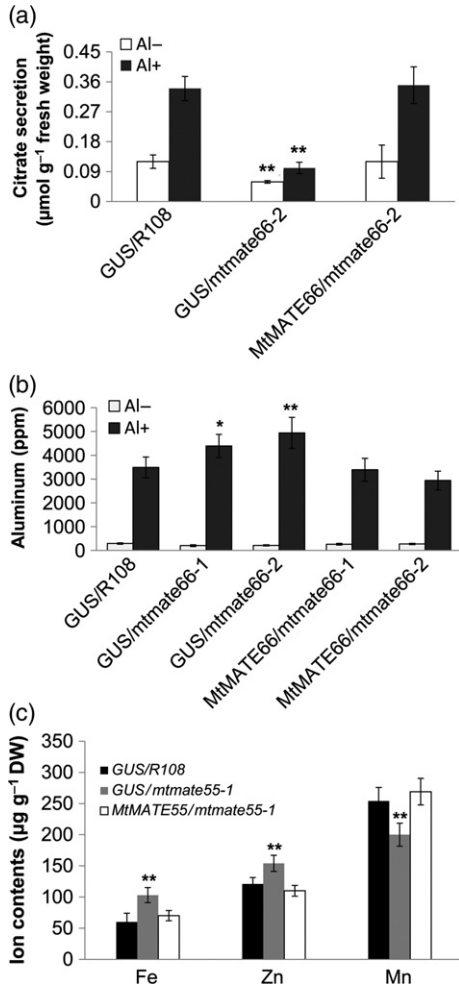


Figure 6. Genetic complementation of *mtmate66* and *mtmate55* mutants. (a) Secretion of citric acid by hairy roots derived from R108 wild-type and *mtmate66-2* plants with overexpressing *GUS* or *MtMATE66*. (b) Al accumulation in the hairy roots derived from R108 wild-type and *mtmate66* mutant plants with overexpressing *GUS* or *MtMATE66* after Al-stress (Al+) or non-stress (Al-) treatment. (c) Fe, Mn and Zn contents in hairy roots derived from R108 wild-type and *mtmate55-1* plants with over-expressing *GUS* or *MtMATE55* under Fe-deficiency conditions. Data are represented as means \pm SDs. Differences between paired data from *GUS* and *MtMATE* overexpression lines in wild-type or different *mtmate* mutant backgrounds under normal (Al-) or Al treatment (Al+ or Fe-) conditions were analyzed by Student's *t*-test ($n = 3$): * $P < 0.05$; ** $P < 0.01$.

quantities of both citric and malic acid secreted into the medium were significantly higher than in the *GUS* control (Figure 7f).

Figure 7. Characterization of *MtSTOP* and transcriptional regulation of *Medicago truncatula* MATE transporters. (a) Phylogenetic tree of C₂H₂ zinc-finger transcription factors related to *MtSTOP*. The phylogenetic tree was constructed by PAUP. Node support was estimated using neighbor-joining bootstrap analysis (1000 bootstrap replicates) to indicate the percentage of consensus support. (b) Expression patterns and induction of *MtSTOP* by H⁺ and Al³⁺ stress, or together. (c) Altered root growth of *MtSTOP* mutants under low pH or low pH plus 50 μ M Al³⁺ stress. (d) Al accumulation in roots of *mtstop-1*, *mtstop-2* under 50 μ M Al³⁺ stress or normal conditions. (e) Citrate secretion from the roots of *mtstop-1*, *mtstop-2* under 50 μ M Al³⁺ stress or normal conditions. (f) Time-course citrate and malate secretion in *MtSTOP* transgenic hairy roots grown under 50 μ M Al³⁺ stress or normal conditions. (g) Expression of *MtMATE55*, *MtMATE66* and *MtMATE69* in *mtstop* mutants and *MtSTOP* overexpression hairy root lines, compared with controls. *MtACTIN* was used as an internal standard; data are represented as means \pm SDs. Differences between paired data from wild-type and *mtstop* mutants or from *GUS* control and *MtSTOP* overexpression lines under normal (Al-) or Al treatment (Al+) conditions were analyzed by Student's *t*-test ($n = 3$): * $P < 0.05$; ** $P < 0.01$. [Colour figure can be viewed at wileyonlinelibrary.com]

MtMATE transporters were regulated by different transcription factors

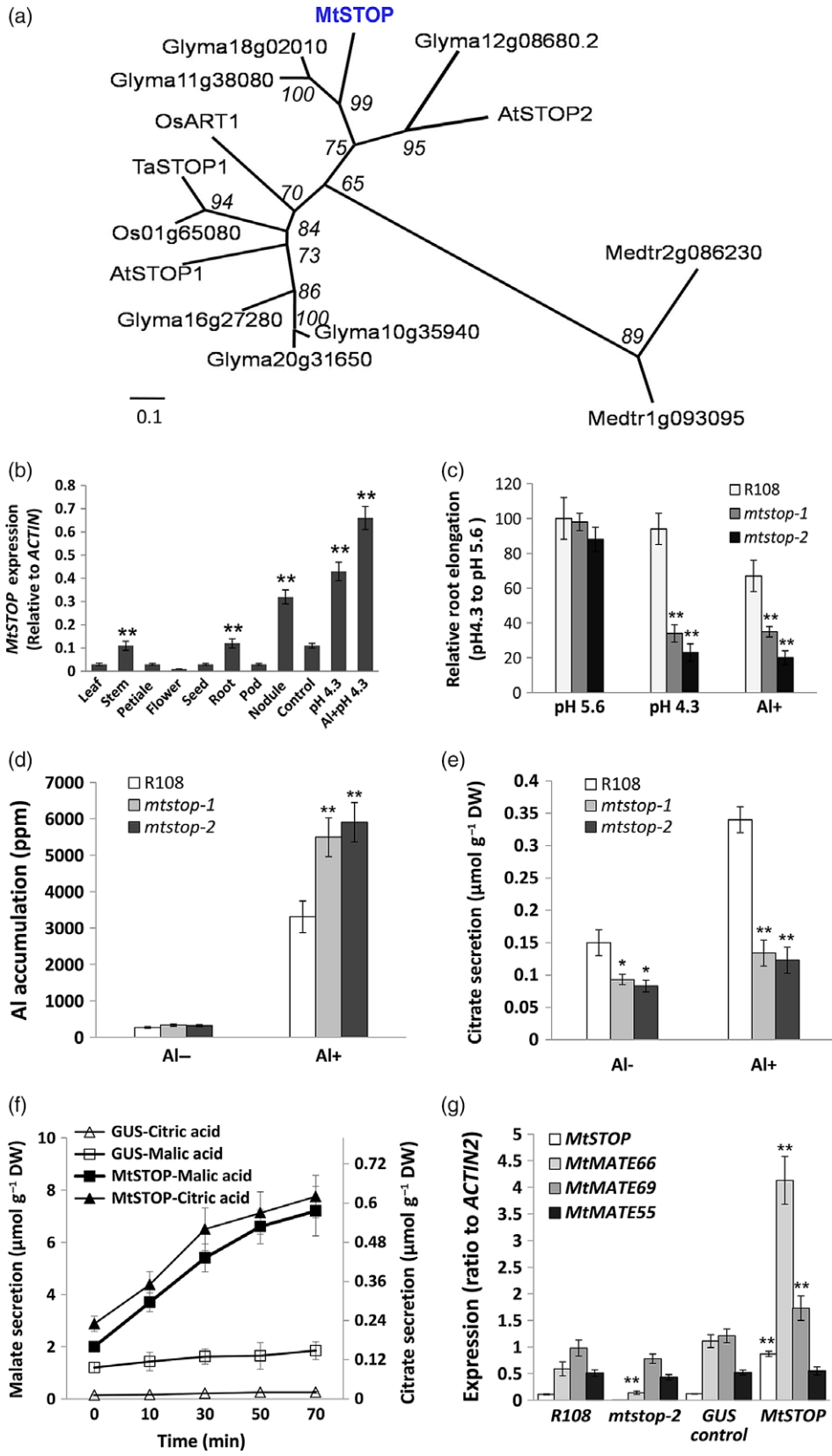
We then examined the effects of *MtSTOP* overexpression on *MATE* gene expression. Overexpression of *MtSTOP* in hairy roots upregulated both *MtMATE66* and *MtALMT69* transcript levels, as well as two putative malate transporters, *MtALMT1* (Medtr7g106260.1) and *MtALMT1* (Medtr2g087288.1). On the other hand, *MtMATE66* expression was dramatically lower in *mtstop-2* mutants, whereas *MtMATE55* and *MtMATE69* expression was unchanged (Figure 7g). Interestingly, the expression of *MtMATE2*, encoding an anthocyanin malonate transporter, was downregulated in flowers of *mtpar*, *mttt8* and *mtwd40-1* mutants (Figure S10). The expression of a proanthocyanidin precursor transporter gene *MtMATE1* was downregulated in *M. truncatula* flowers and seeds of the same mutants (Figure S10). *MtMATE1* and *MtMATE2* were upregulated in hairy roots overexpressing *MtTT8*, *MtPAR*, *MtWD40-1* or *MtLAP1*, with the exception that *MtMATE2* was not induced by *MtPAR* (Figure S10).

Subcellular localization of MtMATE and MtSTOP proteins

We further assessed the subcellular localization of these MtMATE and MtSTOP proteins in order to further understand their physiological roles as membrane transporters or transcription factors. Although we were unable to detect a *MtMATE55-GFP* fusion, the *MtMATE69-GFP* signals mainly localized to the plasma membrane in tobacco epidermal cells (Figure 8b, c), compared with controls expressing GFP alone (Figure 8a). *MtMATE66-GFP* also primarily localized to the plasma membrane when expressed in *M. truncatula* hairy roots (Figure 8d, e). *MtSTOP-GFP* localized to the nucleus, consistent with its potential function as a transcription factor (Figure 8f–h).

DISCUSSION

Through phylogenetic analysis of *Medicago* MATE transporters, we identified several MATE transporters likely to be involved in organic acid secretion and metal ion translocation. We characterized two citrate exporters from distinct phylogenetic subgroups participating in key mechanisms of Al³⁺ tolerance or Fe translocation, and a MATE transporter regulating *Medicago* growth and development and Fe homeostasis in various tissues. These transporters are



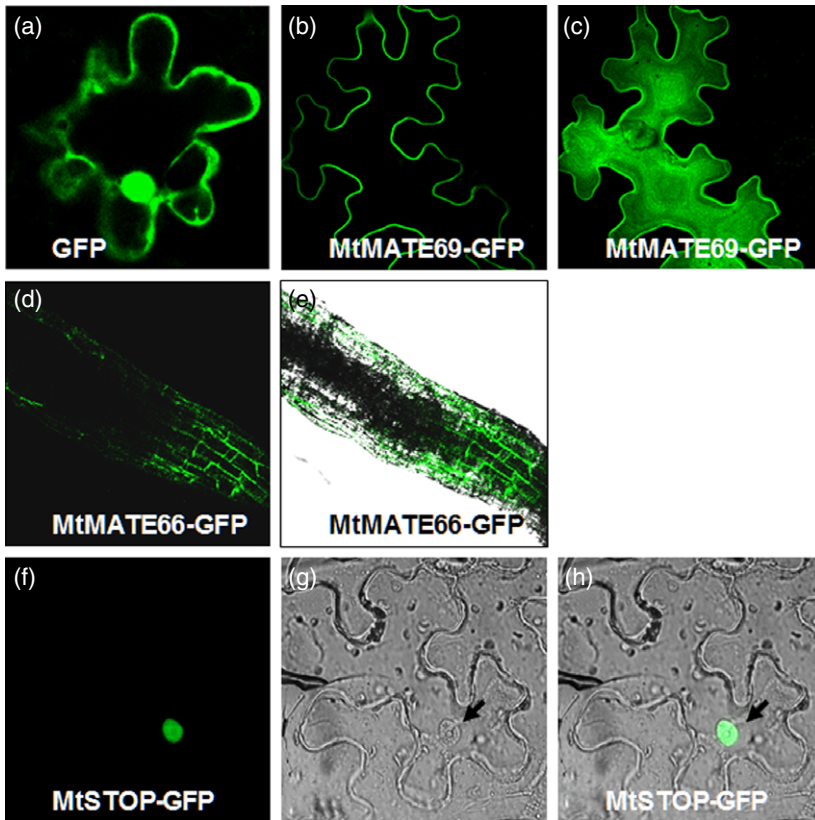


Figure 8. Subcellular localization of MtMATE and MtSTOP in plant cells. (a) Fluorescence image of free GFP. (b) Fluorescence image of MtMATE69-GFP in single-section scanning. (c) Fluorescence image of MtMATE69-GFP projection of 50 optical scanning sections taken at 0.5 μm . (d, e) Fluorescence image of MtMATE66-GFP (d), and the merged image with bright field (e), in transformed hairy roots. (f–h) Fluorescence image (f), bright field (g) and merged image (h) of MtSTOP-GFP. All images are representative of two experiments. Scale bars: 30 μm .

regulated by different transcription factors in response to various environmental and hormonal cues. We further demonstrated that a zinc-finger transcription factor, MtSTOP, plays an important role in activating citrate exporters in roots exposed to H^+ and Al^{3+} toxicity.

Substrate and functional diversity of MATE citric acid efflux transporters

The MATE transporters show affinity to diverse substrates, ranging from metabolic waste xenobiotics, nutrients and secondary metabolites to hormones and signaling molecules. Given the different substrates, tissue-specific expression and varying subcellular localizations, the roles of MATEs in plant physiological and cellular processes are diverse. Plant MATE transporters are often recruited for environmental adaptation (Maron *et al.*, 2010). Al-activated release of organic acids from roots into the rhizosphere or into vascular tissues involves MATE transporters, which are now recognized as a major Al tolerance or Fe translocation mechanism in plants (Kochian *et al.*, 2015). Phylogenetic analysis revealed that MtMATE66 and MtMATE69 are classified into distinct branches, along with homologs from other plant species, despite the fact that they transport the same substrate. Although two groups of plasma membrane MATEs export citric acid out of plant cells, the distinct tissue expression patterns of these two genes in

M. truncatula indicate that they might play different physiological roles. Recent studies have shown that even though two clusters of MATEs have similar transport substrates and subcellular locations, it is the tissue-specific expression, rather than protein structure, that determines their biological functions (Fujii *et al.*, 2012). Citrate transporters, including *FRD3*, *OsFRDL1*, *MtMATE66* and *MtMATE69*, expressed in the vascular tissues of leaves, roots and stems, are required for the root–shoot translocation of metal ions, as their substrates form iron- and zinc-citrate complexes or chelate Al^{3+} to enhance Al tolerance (Durrett *et al.*, 2007; Yokosho *et al.*, 2009; Pineau *et al.*, 2012). In contrast, *AtMATE*, *OsFRDL4* and *MtMATE69* are mainly expressed in root cells, where they are essential for chelating and detoxifying Al^{3+} , or for Fe nutrition (Liu *et al.*, 2009; Yokosho *et al.*, 2011). In addition, both *OsPEZ1* and *OsPEZ2* can participate in Fe translocation by secreting phenolics (Yokosho *et al.*, 2009; Ishimaru *et al.*, 2011). MATE transporters also mediate vacuolar sequestration of polyphenolics and alkaloids (Zhao and Dixon, 2009; Zhao *et al.*, 2011a), as well as ABA and SA, which is indicative of the diverse functions of MATE transporters in plants (Yamasaki *et al.*, 2013; Zhang *et al.*, 2014). MATE proteins have similar substrates and have similar topological structures (Figure S11), suggesting a conserved transport mechanism; however, MATE transporter substrates vary with

topological structure changes (Figure S11). Importantly, substrates of many characterized MATEs have yet to be determined, including ZmBIGE1, AtADS1, AtRHC1, BCD1 (Burko *et al.*, 2011; Seo *et al.*, 2012; Zhang *et al.*, 2014; Suzuki *et al.*, 2015; Wang *et al.*, 2015) and MtMATE55.

MtMATE66 and MtMATE69 are citric acid transporters with overlapping physiological functions

OsFRDL4 and AtMATE1 are responsible for Al-induced citrate secretion by root epidermal cells in rice and Arabidopsis, respectively (Liu *et al.*, 2009; Yokosho *et al.*, 2011). Their ortholog in *M. truncatula*, MtMATE66, is also responsible for both Al³⁺-induced citric acid efflux for Al³⁺ tolerance and Fe nutrition, as demonstrated by its activation by Al³⁺ and enhanced tolerance against Al³⁺ in the genetic complementation of knock-out mutants in *M. truncatula* hairy roots. Similar to *OsFRDL1* and *FRD3*, their Medicago ortholog *MtMATE69* was specifically expressed in root tissues, having a role not only in Fe translocation but also in Al³⁺ tolerance (Durrett *et al.*, 2007; Yokosho *et al.*, 2009). The differential expression patterns of *MtMATE66* and *MtMATE69* may actually be the primary determinant of their physiological functions in Al tolerance and/or Fe translocation, despite their similar subcellular localization and the fact that they have the same substrate. Nevertheless, overexpression of *MtMATE66* resulted in enhanced tolerance to Al stress in *M. truncatula* hairy roots, indicating a potential application in crop breeding for varieties tolerant to Al³⁺ stress in acidic soils.

MtMATE66 may also be expressed in vascular tissues, as suggested by its expression in old stems and roots (Figures S4, S6), indicating that it might have evolved a different function. *mtmate66* mutants showed more severe Fe deficiency symptoms under low-Fe conditions than the wild-type control. The increased expression of *IRT1* and *FRO* homologs under Fe deficiency in overexpression hairy roots and the decreased *FRO* activity in *mtmate66* mutants indicated that MtMATE66 seems to be involved in root uptake of Fe from the soil. *MtMATE66* overexpression also showed Fe over-accumulation compared with the wild type; however, the homologs AtMATE1 and OsFRDL4 have not been reported to have a function in Fe nutrition, probably because they are mostly expressed in root epidermal cells (Liu *et al.*, 2009; Yokosho *et al.*, 2011). Therefore, we posit that MtMATE66 plays two distinct roles, Al³⁺ detoxification and Fe uptake or translocation, with citric acid as the transported substrate.

FRD3 is mainly expressed in root vascular tissues, and is necessary to solubilize iron and zinc in the extracellular space. The *frd3* mutant roots show apoplastic iron deposits, whereas wild-type roots have iron and zinc deposits inside the cells (Pineau *et al.*, 2012). Similarly, we showed that *MtMATE69* overexpression affected Fe and Zn accumulation in *M. truncatula* hairy roots, further suggesting a

function for MtMATE69 in Fe nutrition. Moreover, *MtMATE69* is induced by Al³⁺ stress, and hairy roots overexpressing *MtMATE69* had less Al and better growth, indicating a role for MtMATE69 in Al resistance. Furthermore, MtMATE55 and MtMATE66 loss-of-function mutations or overexpression in hairy roots affected Fe, Zn and Mn homeostases, indicating that both are involved in Fe homeostasis.

MtMATE55, MtMATE66 and MtMATE69 are involved in Fe transport, plant development and growth

All eudicot plants have developed strategy I for the acquisition of Fe as well as other micronutrients from the rhizosphere (Kobayashi and Nishizawa, 2012). Strategy I includes the improvement of the Fe solubility through the release of root exudates, such as H⁺ by plasma membrane H⁺-ATPases, organic acids and phenolic compounds by secondary transporters, and the reduction of Fe³⁺ to the more soluble Fe²⁺ through *FRO* activity in plant roots (Yi and Guerinet, 1996; Robinson *et al.* 1999). Fe²⁺ is then taken up by plant divalent cation transporters, such as *IRT1* (Vert *et al.*, 2002; Kobayashi and Nishizawa, 2012). Both *MtFRO* and *MtIRT1* had different expression profiles in *mtmate* mutants and *MtMATE66* and *MtMATE69* hairy root lines, compared with wild-type and GUS controls, respectively. In addition, *FRO* activity was also consistent with altered *MtMATE66* and *MtMATE69* expression in *M. truncatula*, suggesting probable feedback regulation on *FRO* activity by MtMATEs. Based on these results, MtMATE55 showed different phenotypes from the other two MtMATEs, indicating that they use different mechanisms.

Evolutionary conservation and diversification of MATE transporters are also reflected by the fact that MATE transporters participate in plant development and growth by transporting hormones or signaling molecules in different organs or tissues (Sun *et al.*, 2011, 2011; Zhang *et al.*, 2014; Suzuki *et al.*, 2015; Wang *et al.*, 2015). We showed here that MtMATE55, an ortholog of BCD1 that is involved in Fe translocation and apical development (Seo *et al.*, 2012), was also involved in Fe homeostasis and seedling development, architecture and growth; however, MtMATE55 evidently affected Fe homeostasis in a way that is somewhat different from its Arabidopsis ortholog, although the substrates and mechanisms underlying the functions of both are yet to be determined. The phenotypes of *mtmate55* mutants and overexpressing transgenic roots are not exactly same as those of the *bcd1* mutant in terms of Fe fluctuations, compared with wild-type controls. For instance, compared with *bcd1* under Fe-deficient and over-supplied conditions, the Fe content in shoot and root tissues of *mtmate55* seedlings and *MtMATE55*-overexpressing roots are different (Seo *et al.*, 2012). The altered hormones in these mutants and overexpression hairy roots provided clues as to how these MATE transporters affect

root elongation and seedling development by indirectly affecting hormone levels. Previous studies have indicated that Fe or Al³⁺ stress regulates the synthesis, transport and signaling of auxin and other hormones, through which they inhibit root development (Yang *et al.*, 2014; Li *et al.*, 2015a). Indeed, auxin and other stress hormones, such as ethylene, ABA and SA, can regulate metal distribution, stress responses and plant tolerance to stress (Zhu *et al.*, 2013). Here, we show that MtMATEs also participate in the plant response to metal stresses, together with altered hormones, although the precise relationships between these two systems remain elusive. In particular, the intriguing relationship between MtMATE55 and ABA accumulation warrants further investigation.

Transcriptional regulation of MATE transporters by conserved mechanisms

Little is known about the molecular mechanisms regulating the expression of MATE transporters at the transcriptional or translational levels (Delhaize *et al.*, 2012). In Arabidopsis, AtSTOP1, a C₂H₂-type zinc-finger transcription factor, induces the expression of AtMATE1 in roots in response to Al³⁺ stress (Liu *et al.*, 2009). Similarly, the rice AtSTOP1 homolog, OsART1, regulates *OsFRDL4* (Tsutsui *et al.*, 2011; Yokosho *et al.*, 2011). AtSTOP2 also regulates additional genes that protect Arabidopsis roots from H⁺ and Al³⁺ toxicity (Ohya *et al.*, 2013; Kobayashi *et al.*, 2014). In *M. truncatula*, MtSTOP was shown to have a similar function in regulating plant responses to acidic and Al³⁺ stresses. For unknown reasons, we identified no functionally active AtSTOP1 homolog in *M. truncatula*. Our data suggest that MtSTOP regulates *MtMATE66*. As such, it participates in the regulation of Medicago physiological responses against H⁺ and Al³⁺ toxicity. Except for proanthocyanidin synthetic genes that are regulated by a MYB-bHLH-WD40 ternary complex (Li *et al.*, 2016), our study demonstrated that *MtMATE1* in developing seeds and *MtMATE2* in flowers are regulated by MtPAR, MtLAP1, MtTT8 and MtWD40-1 transcription factors (Zhao *et al.* 2011a; Zhao, 2015).

In summary, the present study sheds light on our understanding of the diverse roles of the MATE transporter family in physiological responses to H⁺ and Al toxicities in plants, which may present valuable information that is useful in molecular breeding and evolutionary studies.

EXPERIMENTAL PROCEDURES

Plant materials and *Tnt1* insertion mutant screening

Medicago truncatula *Tnt1* insertional mutants in the ecotype R108 background were used for all experiments. *Tnt1* retrotransposon insertions into *MtMATE55*, *MtMATE66* and *MtSTOP* genes were identified as described previously, using a nested PCR approach (Tadege *et al.*, 2008). *Tnt1* flanking sequences were retrieved from the *M. truncatula* mutant database (<http://medicago-mutant.noble.org/mutant>) and confirmed by PCR with a combination of *MtMATE* gene-specific and *Tnt1*-specific primers (Table S8). *Tnt1* insertion sites in *MtMATE* genes were verified by sequencing. Other mutant lines were identified *in silico* through analyses of *Tnt1* flanking sequences in the mutant population (<http://bioinfo4.noble.org/mutant/line2.php>). Loss or reduction of *MtMATE* transcription in homozygous lines of four independent *Tnt1* mutants was confirmed by qRT-PCR using gene- and *Tnt1*-specific primers (Table S8). Homozygous *M. truncatula* plants were obtained from these *Tnt1* mutant populations after three rounds of segregation, and were tested for the following gene insertions: NF5006 (*mtmate66-1*), NF11176 (*mtmate66-2*), NF0245 (*mtmate55-1*), NF5453 (*mtstop-1*) and NF7132 (*mtstop-2*). The *Tnt1* mutants for *mtwd40-1*, *mttt8* and *mtpar* used in this work have been described previously (Li *et al.*, 2016).

Seeds from the identified *Tnt1* insertion lines were scarified for 10 min with concentrated sulfuric acid, washed three times, cold-treated for 3 days at 4°C on filter paper, and grown in a glasshouse on Metro-Mix 350 with an 18-h light/25°C and 6-h dark/22°C photoperiod. Verification of the presence of *Tnt1* insertions in an individual plant and analysis of its homozygous or heterozygous status were based on the presence or absence of amplification products. The impact of the *Tnt1* insertion on gene transcription was verified by RT-PCR using gene-specific primers.

Seeds from the identified *Tnt1* insertion lines were scarified for 10 min with concentrated sulfuric acid, washed three times, cold-treated for 3 days at 4°C on filter paper, and grown in a glasshouse on Metro-Mix 350 with an 18-h light/25°C and 6-h dark/22°C photoperiod. Verification of the presence of *Tnt1* insertions in an individual plant and analysis of its homozygous or heterozygous status were based on the presence or absence of amplification products. The impact of the *Tnt1* insertion on gene transcription was verified by RT-PCR using gene-specific primers.

Construction of MtMATE and MtSTOP vectors

Open reading frames of *MtMATE66*, *MtMATE69*, *MtMATE55* and *MtSTOP* were amplified from cDNA prepared from total RNA isolated from *M. truncatula* root or leaf tissues (primers listed in Table S8) using a high-fidelity Taq DNA polymerase (New England Biolabs, <http://www.neb.com>). PCR products were cloned into the Gateway Entry vector pENTR/D-TOPO (Invitrogen, now ThermoFisher Scientific, <https://www.thermofisher.com>), and the resulting vectors, pENTR-MtMATEs or pENTR-MtSTOP, were confirmed by sequencing. The entry vectors were used to construct binary vectors using Gateway recombination technology (ThermoFisher Scientific) into the pB7WG2D plant expression vector, along with a GFP marker, to transform *M. truncatula* hairy roots. For each gene under study, entry vectors were recombined into the pB2GW7 destination vector for constitutive expression driven by the 35S promoter for complementation of the corresponding *M. truncatula* mutants. The *GUS* gene was used as a control for both vectors.

Epitopic expression of MtMATEs and MtSTOP

The pB7WG2D binary vectors, harboring *MtMATE55*, *MtMATE66*, *MtMATE69* and *MtSTOP*, as well as *GUS* as a control, were transformed into the *Agrobacterium rhizogenes* strain ARqua1 by electroporation (Li *et al.*, 2016). Transformed colonies were grown at 28°C on an LB agar medium supplied with spectinomycin and streptomycin. After confirmation by PCR, *Agrobacteria* were used to infiltrate leaves from both wild-type *M. truncatula* and the corresponding *MtMATE* and *MtSTOP* mutant plants: NF11176 (*mtmate66-2*), NF0245 (*mtmate55-1*) and NF7132 (*mtstop-2*) (Li *et al.*, 2016). Samples were collected for RNA extraction as previously described (Li *et al.*, 2016).

Medicago truncatula hairy roots expressing pB2GW7-*MtMATE55*, pB2GW7-*MtMATE66*, pB2GW7-*MtMATE69* and pB2GW7-*MtSTOP*, as well as the pB2GW7-*GUS* control, were transferred into liquid medium [pH 4.3, buffered with 5 mM 2-(*N*-morpholino)ethanesulfonic acid (MES)] containing 50 μM AlCl₃ for a time-course study. For genetic complementation, hairy root lines of *mtmate66-2* mutant roots expressing *MtMATE66*,

mtmate55-1 expressing *MtMATE55*, as well as *mtstop-2* expressing *MtSTOP* were treated similarly in a time-course study. Root exudates were collected by exposing transgenic hairy roots grown in liquid medium, washing them thoroughly with deionized water and then exposing the roots for 24 h to an MES-buffered medium (pH 4.3) containing 0.5 μM CaCl_2 and 50 μM AlCl_3 . Samples were harvested and snap frozen for RNA extraction.

RNA isolation and analysis

Total RNA was extracted from samples using the RNeasy plant mini kit or Trizol reagents, according to the manufacturer's instructions (Qiagen, <http://www.qiagen.com>; Li *et al.*, 2016). Quantitative RT-PCR was performed as described previously (Zhao *et al.*, 2011a).

pH, Al^{3+} and Fe treatments of plants and hairy roots

For citric acid secretion assays, *mtmate55*, *mtmate66* or *mtstop* mutants and wild-type control seedlings or *GUS* hairy roots controls were transferred to fresh medium (pH 4.3) with 0 or 50 μM Al^{3+} for 0, 15 and 30 min, as well as for 1, 2 and 3 days of exposure. Hairy roots exposed to medium without Al^{3+} were used as a control. For testing the effect of pH, sterile R108 and *mtstop* mutant seeds were germinated in a medium buffered to pH 5.6 for 10 days before being transferred to acidic medium (pH 4.3). The composition of the medium at pH 5.6 was identical to that of the acidic medium (pH 4.3), except that MES was omitted. R108 and *mtstop* seedlings were transferred to acidic medium supplemented with 0 or 50 μM Al^{3+} for an additional 1, 3 or 6 days. For growth assays, hairy roots and seedlings were treated under similar conditions for 3 days as described above. Roots were rinsed with distilled water, wiped gently with paper towels, measured for fresh weight and immediately frozen in liquid nitrogen. For Fe treatments, iron-sufficient media were standard half-strength MS medium supplemented with 0.05% MES, 1% sucrose and 50 μM Fe-EDTA, instead of iron sulfate as in the original MS recipe (Murashige & Skoog, 1962). Iron-deficient media were prepared by including 300 μM ferrozine instead of iron sulfate. For treatments using excessive iron, 400 μM FeSO_4 was added to the fresh liquid medium, as previously described (Yokosho *et al.*, 2009, 2011).

Measurement of chlorophyll content, root elongation, and Al, Fe and Zn content

Ten-day-old seedlings of both wild type and *mtmate* mutant lines were treated and assayed for root elongation as previously described (Zhao *et al.*, 2015). The chlorophyll content of leaves was measured as previously described (Zhao *et al.*, 2015). Ion concentrations were measured using ICP-MS as previously described (Zhao *et al.*, 2011b). The organic acid exuded from roots was analyzed to determine the profiles of organic acids as previously described (Zhao *et al.*, 2011b). Hormones were extracted and measured by using LC-MS with a method previously described (Pan *et al.*, 2010).

Root Fe(III) reduction activity assay

Single intact hairy roots overexpressing *MtMATEs* or intact roots of *mtmate* mutants were evaluated for Fe^{3+} reduction activity. *M. truncatula* roots or hairy roots were assayed according to methods described previously (Yi and Gueriot, 1996). In brief, roots were incubated in the dark at room temperature (25°C) for 1 h in an aerated buffer containing 0.1 mM Fe(III) EDTA, 0.3 mM Ferrozine, pH 6.5, adjusted with MES-KOH to a final strength of

10 mM. The absorbance at 562 nm was measured at 30-min intervals. The concentration of the Fe(II)–Ferrozine complex formed by the reduction of Fe^{3+} was calculated by using an extinction coefficient of 28.6 $\text{mm}^{-1} \text{cm}^{-1}$.

Subcellular localization analyses

The green fluorescent protein (GFP) coding sequence was fused in frame to the 5' end of the *MATE* genes under study, and each fragment was subcloned into the pGFP vector (Zhao *et al.*, 2011a). The fusion construct was delivered either by tobacco leaf infiltration with *A. tumefaciens* EHA105 or transformed into *M. truncatula* hairy roots by *A. rhizogenes* strain *ARqua1*. Imaging of GFP and GFP fusion proteins was performed with a Leica TCS SP2 inverted confocal microscope using a 63 \times water-immersion objective and Leica CONFOCAL software (<http://www.leica.com>). Serial optical sections of 0.5 μm were obtained at a resolution of 512 \times 512 pixels using an excitation wavelength of 488 nm, and emissions were collected between 500 and 560 nm and analyzed using Leica LAS AF software.

Bioinformatics analysis

Cluster analyses used Affymetrix microarray-based gene expression data obtained from Medicago Gene Atlas (<http://mtgea.noble.org/v3>). Expression data were log₂ transformed, and hierarchical clustering was conducted based on Pearson correlations using MEV 4.0. Statistical verification of the probabilities for root expression data was determined using PVCLUST (Li *et al.*, 2016). Gene expression data for the flavonoid and lignin mutants (*mtwd40-1*, *mttt8*, *mtpar*, *ccr1*, *cad1*, *hct1*, *4cl*, *c3h* and *nst*) were described previously (Zhao *et al.*, 2010, 2013; Zhou *et al.*, 2010; Gallego-Giraldo *et al.*, 2011; Li *et al.*, 2016). The accession numbers were: MtMATE2 (HM856605), MtMATE1 (ACX37118), MtMATE55 (KT878752), MtMATE66 (KT878753), MtMATE69 (KT878754) and MtSTOP (KT878755); MtIRT1 (KX641478), MtALMT1 (KX641479), MtALMT2 (KX641480); and MtFRO1 (KX641481); MtFRO2 (KX641482).

Statistical analyses

In most experiments, at least three independent experiments with duplicates were performed. Differences between paired data from wild-type and mutant plants or from *GUS* control and *MtMATE* or *MtSTOP* overexpression lines under normal (Al[−] or Fe⁺) or stress treatment (Al⁺ or Fe[−]) conditions were analyzed by Student's *t*-test ($n = 3$); * $P < 0.05$; ** $P < 0.01$. The differences between two tails of data with the error bars represent 95% confidence limits.

ACKNOWLEDGEMENTS

We are grateful to Dr Richard A. Dixon for his kind support in the initiation of this work, Dr Yuhong Tang for computational analysis and Dr David Salt's Lab for part of the ionic analysis. We would also thank Dr Adrienne R. Washington for her editorial revision of this manuscript. This work was supported by the Ministry of Science and Technology of China (grant 2016YFD0100504) and the Major State Basic Research Development Program of China (973 Program 2013CB127001), and the Fundamental Research Funds for the Central Universities (2013PY065). The authors declare no conflicts of interest.

AUTHORS' CONTRIBUTIONS

J.Z. planned and designed the research; J.W., Q.H., J.Z., P.L., B.C. and X.F. performed experiments and analyzed data;

X.S. conducted ionomic analysis; V.A.B. and L.Y. conducted bioinformatic analyses and the curation of the MATE family; J.W. and K.S.M. created and provided Tnt1 mutants; and J.Z. and V.A.B. wrote and edited the manuscript.

SUPPORTING INFORMATION

Additional Supporting Information may be found in the online version of this article.

Figure S1. Synteny of MtMATEs in *Medicago truncatula* and Arabidopsis genomes.

Figure S2. Expression profile of *MtMATE55*.

Figure S3. Expression heat map of *Medicago truncatula* MATE transporters.

Figure S4. Expression profiles of *MtMATE66* and *MtMATE69*.

Figure S5. Phylogeny and expression analysis of MtMATE transporters involved in organ development and growth.

Figure S6. Expression of *MtMATE* genes in response to salt, drought and AlCl₃ stress.

Figure S7. Expression profile of *MtSTOP*.

Figure S8. Identification of Fe(III) reduction oxidase and IRT1 from *M. truncatula*.

Figure S9. Analysis of lignin contents in stems of the *mtmate55-1* mutant and the wild-type plant.

Figure S10. Transcriptional regulation of *M. truncatula* MATE transporter genes.

Figure S11. Topological analysis of MtMATEs compared with homologous MATEs characterized in other plants.

Table S1. Tandem duplications and syntenic paralogs of MATE transporter genes in the *Medicago truncatula* genome.

Table S2. Tandem duplications and syntenic paralogs of MATE transporter genes in the *Medicago truncatula* and Arabidopsis genomes.

Table S3. BlastN analysis of *Tnt1* flanking sequences retrieved from mutant NF5006 (*mtmate66-1*).

Table S4. BlastN analysis of *Tnt1* flanking sequences retrieved from mutant NF11176 (*mtmate66-2*).

Table S5. BlastN analysis of *Tnt1* flanking sequences retrieved from mutant NF0245 (*mtmate55-1*).

Table S6. BlastN analysis of *Tnt1* flanking sequences retrieved from mutant NF5453 (*mtstop-1*).

Table S7. BlastN analysis of *Tnt1* flanking sequences retrieved from mutant NF7132 (*mtstop-2*).

Table S8. Primers used in the study.

Appendix S1. Sequences of identified MATE transporters in the *Medicago truncatula* genome.

Appendix S2. Curated list of MATE transporters from the *Medicago truncatula* genome version 4.0.

REFERENCES

- Bashir, K., Ishimaru, Y., Shimo, H. *et al.* (2011) Rice phenolics efflux transporter 2 (PEZ2) plays an important role insolubilizing apoplasmic iron. *Soil Sci. Plant Nutr.* **57**, 803–812.
- Benedito, V.A., Torres-Jerez, I., Murray, J.D. *et al.* (2008) A gene expression atlas of the model legume *Medicago truncatula*. *Plant J.* **55**, 504–513.
- Brown, M.H., Paulsen, I.T. and Skurray, R.A. (1999) The multidrug efflux protein NorM is a prototype of a new family of transporters. *Mol. Microbiol.* **31**, 394–395.
- Burko, Y., Geva, Y., Refael-Cohen, A., Shleizer-Burko, S., Shani, E., Berger, Y., Halon, E., Chuck, G., Moshelion, M. and Ori, N. (2011) From organelle to organ: ZRIZI MATE-type transporter is an organelle transporter that enhances organ initiation. *Plant Cell Physiol.* **52**, 518–527.
- Chandran, D., Sharopova, N., VandenBosch, K.A., Garvin, D.F. and Samac, D.A. (2008) Physiological and molecular characterization of aluminum resistance in *Medicago truncatula*. *BMC Plant Biol.* **8**, 89.
- Delhaize, E., Ma, J. and Ryan, P.R. (2012) Transcriptional regulation of aluminum tolerance genes. *Trends Plant Sci.* **17**, 341–348.
- Diener, A.C., Gaxiola, R.A. and Fink, G.R. (2001) Arabidopsis *ALF5*, a multidrug efflux transporter gene family member, confers resistance to toxins. *Plant Cell*, **13**, 1625–1638.
- Dobritzsch, M., Lübken, T., Eschen-Lippold, L., Gorzalka, K., Blum, E., Matern, A., Marillonnet, S., Böttcher, C., Dräger, B. and Rosahl, S. (2016) MATE transporter-dependent export of hydroxycinnamic acid amides. *Plant Cell*, **28**, 583–596.
- Durrett, T.P., Gassmann, W. and Rogers, E.E. (2007) The FRD3-mediated efflux of citrate into the root vasculature is necessary for efficient iron translocation. *Plant Physiol.* **144**, 197–205.
- Fujii, M., Yokosho, K., Yamaji, N., Saisho, D., Yamane, M., Takahashi, H., Sato, K., Nakazono, M. and Ma, J.F. (2012) Acquisition of aluminium tolerance by modification of a single gene in barley. *Nat. Commun.* **3**, 132–136.
- Gallego-Giraldo, L., Jikumaru, Y., Kamiya, Y., Tang, Y. and Dixon, R.A. (2011) Selective lignin downregulation leads to constitutive defense response expression in alfalfa (*Medicago sativa* L.). *New Phytol.* **190**, 627–639.
- Green, L. and Rogers, E.E. (2004) FRD3 controls iron localization in Arabidopsis. *Plant Physiol.* **136**, 2523–2531.
- Hoekenga, O.A., Maron, L.G., Pineros, M.A. *et al.* (2006) AtALMT1, which encodes a malate transporter, is identified as one of several genes critical for aluminum tolerance in Arabidopsis. *Proc. Natl Acad. Sci. USA*, **103**, 9738–9743.
- Ishimaru, Y., Kakei, Y., Shimo, H., Bashir, K., Sato, Y., Sato, Y., Uozumi, N. and Nishizawa, N.K. (2011) A rice phenolic efflux transporter is essential for solubilizing precipitated apoplasmic iron in the plant stele. *J. Biol. Chem.* **286**, 24649–24655.
- Iuchi, S., Koyama, H., Iuchi, A., Kobayashi, Y., Kitabayashi, S., Kobayashi, Y., Ikka, T., Hirayama, T., Shinozaki, K. and Kobayashi, M. (2007) Zinc finger protein STOP1 is critical for proton tolerance in Arabidopsis and coregulates a key gene in aluminum tolerance. *Proc. Natl Acad. Sci. USA*, **104**, 9900–9905.
- Kobayashi, T. and Nishizawa, N.K. (2012) Iron uptake, translocation, and regulation in higher plants. *Annu. Rev. Plant Biol.* **63**, 131–152.
- Kobayashi, Y., Ohyama, Y., Kobayashi, Y. *et al.* (2014) STOP2 activates transcription of several genes for Al- and low pH-tolerance that are regulated by STOP1 in Arabidopsis. *Mol. Plant*, **7**, 311–322.
- Kochian, L.V., Pineros, M.A., Liu, J. and Magalhaes, J.V. (2015) Plant adaptation to acid soils: the molecular basis for crop aluminum resistance. *Annu. Rev. Plant Biol.* **66**, 571–598.
- Kuroda, T. and Tsuchiya, T. (2009) Multidrug efflux transporters in the MATE family. *Biochim. Biophys. Acta*, **1794**, 763–768.
- Li, L., He, Z., Pandey, G.K., Tsuchiya, T. and Luan, S. (2002) Functional cloning and characterization of a plant efflux carrier for multidrug and heavy metal detoxification. *J. Biol. Chem.* **277**, 5360–5368.
- Li, G., Song, H., Li, B., Kronzucker, H.J. and Shi, W. (2015a) Auxin resistant1 and PIN-FORMED2 protect lateral root formation in Arabidopsis under iron Stress. *Plant Physiol.* **169**, 2608–2623.
- Li, J., Li, R., Jiang, Z., Gu, H. and Qu, L. (2015b) ADP1 affects abundance and endocytosis of PIN-FORMED proteins in Arabidopsis. *Plant Signal. Behav.* **10**, 1559–2324.
- Li, P., Chen, B., Zhang, G., Chen, L., Dong, Q., Wen, J., Mysore, K.S. and Zhao, J. (2016) Regulation of anthocyanin and proanthocyanidin biosynthesis by *Medicago truncatula* bHLH transcription factor MtTT8. *New Phytol.* **201**, 905–921.
- Liang, C., Pineros, M.A., Tian, J., Yao, Z., Sun, L., Liu, J., Shaff, J., Coluccio, A., Kochian, L.V. and Liao, H. (2013) Low pH, aluminum, and phosphorus coordinately regulate malate exudation through GmALMT1 to improve soybean adaptation to acid soils. *Plant Physiol.* **161**, 1347–1361.
- Liu, J., Magalhaes, J.V., Shaff, J. and Kochian, L.V. (2009) Aluminum-activated citrate and malate transporters from the MATE and ALMT families function independently to confer Arabidopsis aluminum tolerance. *Plant J.* **57**, 389–399.
- Liu, J., Li, Y., Wang, W., Gai, J. and Li, Y. (2016) Genome-wide analysis of MATE transporters and expression patterns of a subgroup of MATE genes in response to aluminum toxicity in soybean. *BMC Genom.* **17**, 223.
- Magalhaes, J.V., Liu, J., Guimarães, C.T. *et al.* (2007) A gene in the multidrug and toxic compound extrusion (MATE) family confers aluminum tolerance in sorghum. *Nat. Genet.* **39**, 1156–1161.

- Maron, L.G., Piñeros, M.A., Guimaraes, C.T., Magalhaes, J.V., Pleiman, J.K., Mao, C., Shaff, J., Belicuas, S.N.J. and Kochian, L.V. (2010) Two functionally distinct members of the MATE (multi-drug and toxic compound extrusion) family of transporters potentially underlie two major aluminum tolerance QTLs in maize. *Plant J.* **61**, 728–740.
- Morita, Y., Kodama, K., Shiota, S., Mine, T., Kataoka, A., Mizushima, T. and Tsuchiya, T. (1998) NorM, a putative multidrug efflux protein, of *Vibrio parahaemolyticus* and its homolog in *Escherichia coli*. *Antimicrob. Agents Chemother.* **42**, 1778–1782.
- Moriyama, Y., Hiasa, M., Matsumoto, T. and Omote, H. (2008) Multidrug and toxic compound extrusion (MATE)-type proteins as anchor transporters for the excretion of metabolic waste products and xenobiotics. *Xenobiotica*, **38**, 1107–1118.
- Murashige, T. and Skoog, F. (1962) A revised medium for rapid growth and bioassays with tobacco cultures. *Physiol. Plant*, **15**, 473–497.
- Ohyama, Y., Ito, H., Kobayashi, Y. et al. (2013) Characterization of AtSTOP1 orthologous genes in tobacco and other plant species. *Plant Physiol.* **162**, 1937–1946.
- Omote, H., Hiasa, M., Matsumoto, T., Otsuka, M. and Moriyama, Y. (2006) The MATE proteins as fundamental transporters of metabolic and xenobiotic organic cations. *Trends Pharmacol. Sci.* **11**, 587–593.
- Pan, X., Welti, R. and Wang, X. (2010) Quantitative analysis of major plant hormones in crude plant extracts by high-performance liquid chromatography-mass spectrometry. *Nat. Protoc.* **5**, 986–992.
- Pineau, C., Loubet, S., Lefoulon, C., Challes, C., Fizames, C., Lacombe, B., Ferrand, M., Loudet, O., Berthomieu, P. and Richard, O. (2012) Natural variation at the *FRD3* MATE transporter locus reveals cross-talk between Fe homeostasis and Zn tolerance in *Arabidopsis thaliana*. *PLoS Genet.* **8**, e1003120.
- Ren, Q. and Paulsen, I.T. (2005) Comparative analysis of fundamental differences in membrane transport capabilities in prokaryotes and eukaryotes. *PLoS Comput. Biol.* **1**, e27.
- Robinson, N.J., Procter, C.M., Connolly, E.L. and Guerinot, M.L. (1999) A ferric-chelate reductase for iron uptake from soils. *Nature*. **397**, 694–697.
- Saier, M.H. Jr and Paulsen, I.T. (2001) Phylogeny of multidrug transporters. *Semin. Cell Dev. Biol.* **12**, 205–213.
- Seo, P.J., Park, J., Park, M.J., Kim, Y.S., Kim, S.G., Jung, J.H. and Park, C.M. (2012) A Golgi-localized MATE transporter mediates iron homeostasis under osmotic stress in *Arabidopsis*. *Biochem. J.* **442**, 551–561.
- Serrano, M., Wang, B., Aryal, B., Garcion, C., Abou-Mansour, E., Heck, S., Geisler, M., Mauch, F., Nawrath, C. and Métraux, J.P. (2013) Export of salicylic acid from the chloroplast requires the multidrug and toxin extrusion-like transporter EDS5. *Plant Physiol.* **162**, 1815–1821.
- Sun, X., Gilroy, E.M., Chini, A., Nurnberg, P.L., Hein, I., Lacomme, C., Birch, P.R., Hussain, A., Yun, B.W. and Loake, G.J. (2011) *ADS1* encodes a MATE-transporter that negatively regulates plant disease resistance. *New Phytol.* **192**, 471–482.
- Suzuki, M., Sato, Y., Wu, S., Kang, B.H. and McCarty, D.R. (2015) Conserved functions of the MATE transporter BIG EMBRYO1 in regulation of lateral organ size and initiation rate. *Plant Cell*, **27**, 2288–2300.
- Tadege, M., Wen, J., He, J. et al. (2008) Large-scale insertional mutagenesis using the *Tnt1* retrotransposon in the model legume *Medicago truncatula*. *Plant J.* **54**, 335–347.
- Takanashi, K., Yokosho, K., Saeki, K., Sugiyama, A., Sato, S., Tabata, S., Ma, J. and Yazaki, K. (2013) LjMATE1: a citrate transporter responsible for iron supply to the nodule infection zone of *Lotus japonicus*. *Plant Cell Physiol.* **54**, 585–594.
- Tian, W., Hou, C., Ren, Z. et al. (2015) A molecular pathway for CO₂ response in *Arabidopsis* guard cells. *Nat. Commun.* **6**, 6057.
- Tokizawa, M., Kobayashi, Y., Saito, T., Kobayashi, M., Iuchi, S., Nomoto, M., Tada, Y., Yamamoto, Y.Y. and Koyama, H. (2015) SENSITIVE TO PROTON RHIZOTOXICITY1, CALMODULIN BINDING TRANSCRIPTION ACTIVATOR2, and other transcription factors are involved in ALUMINIUM-ACTIVATED MALATE TRANSPORTER1 expression. *Plant Physiol.* **167**, 991–1003.
- Tsutsui, T., Yamaji, N. and Ma, J. (2011) Identification of a cis-acting element of *ART1*, a C2H2-type zinc-finger transcription factor for aluminum tolerance in rice. *Plant Physiol.* **156**, 925–931.
- Vert, G., Grotz, N., Dédaldéchamp, F., Gaymard, F., Guerinot, M.L., Briat, J.F. and Curie, C. (2002) IRT1, an Arabidopsis transporter essential for iron uptake from the soil and for plant growth. *Plant Cell*, **14**, 1223–1233.
- Wang, R., Liu, X., Liang, S., Ge, Q., Li, Y., Shao, J., Qi, Y., An, L. and Yu, F. (2015) A subgroup of MATE transporter genes regulates hypocotyl cell elongation in *Arabidopsis*. *J. Exp. Bot.* **66**, 6327–6343.
- Yamaji, N., Huang, C.F., Nagao, S., Yano, M., Sato, Y., Nagamura, Y. and Ma, J.F. (2009) A zinc finger transcription factor ART1 regulates multiple genes implicated in aluminum tolerance in rice. *Plant Cell*, **21**, 3339–3349.
- Yamasaki, K., Motomura, Y., Yagi, Y., Nomura, H., Kikuchi, S., Nakai, M. and Shiina, T. (2013) Chloroplast envelope localization of EDS5, an essential factor for salicylic acid biosynthesis in *Arabidopsis thaliana*. *Plant Signal. Behav.* **8**, e23603.
- Yang, Z.B., Geng, X., He, C., Zhang, F., Wang, R., Horst, W.J. and Ding, Z. (2014) TAA1-regulated local auxin biosynthesis in the root-apex transition zone mediates the aluminum-induced inhibition of root growth in *Arabidopsis*. *Plant Cell*, **26**, 2889–2904.
- Yazaki, K. (2005) Transporters of secondary metabolites. *Curr. Opin. Plant Biol.* **8**, 301–307.
- Yi, Y. and Guerinot, M.L. (1996) Genetic evidence that induction of root Fe (III) chelate reductase activity is necessary for iron uptake under iron deficiency. *Plant J.* **10**, 835–844.
- Yokosho, K., Yamaji, N., Ueno, D., Mitani, N. and Ma, J. (2009) OsFRDL1 is a citrate transporter required for efficient translocation of iron in rice. *Plant Physiol.* **149**, 297–305.
- Yokosho, K., Yamaji, N. and Ma, J. (2011) An Al-inducible MATE gene is involved in external detoxification of Al in rice. *Plant J.* **68**, 1061–1069.
- Young, N.D., Debellé, F., Oldroyd, G.E. et al. (2011) The Medicago genome provides insight into the evolution of rhizobial symbioses. *Nature*, **480**, 520–524.
- Zhang, H., Zhu, H., Pan, Y., Yu, Y., Luan, S. and Li, L. (2014) A DTX/MATE-type transporter facilitates abscisic acid efflux and modulates ABA sensitivity and drought tolerance in *Arabidopsis*. *Mol. Plant*, **7**, 1522–1532.
- Zhao, J. (2015) Flavonoid transport mechanisms: how to go, and with whom. *Trends Plant Sci.* **20**, 576–585.
- Zhao, J. and Dixon, R.A. (2009) MATE transporters facilitate vacuolar uptake of epicatechin 3'-O-glucoside for proanthocyanidin biosynthesis in *Medicago truncatula* and *Arabidopsis*. *Plant Cell*, **21**, 2323–2340.
- Zhao, Q., Gallego-Giraldo, L., Wang, H., Zeng, Y., Ding, S.Y., Chen, F. and Dixon, R.A. (2010) An NAC transcription factor orchestrates multiple features of cell wall development in *Medicago truncatula*. *Plant J.* **63**, 100–114.
- Zhao, J., Huhman, D., Shadle, G., He, X., Sumner, L.W., Tang, Y. and Dixon, R.A. (2011a) MATE2 mediates vacuolar sequestration of flavonoid glycosides and glycoside malonates in *Medicago truncatula*. *Plant Cell*, **23**, 1536–1555.
- Zhao, J., Wang, C., Bedair, M., Welti, R., Sumner, L.W., Baxter, B. and Wang, X. (2011b) Suppression of phospholipase D_γs confers increased aluminum resistance in *Arabidopsis thaliana*. *PLoS ONE*, **6**, e28086.
- Zhao, Q., Tobimatsu, Y., Zhou, R. et al. (2013) Loss of function of cinnamyl alcohol dehydrogenase 1 leads to unconventional lignin and a temperature-sensitive growth defect in *Medicago truncatula*. *Proc. Natl Acad. Sci. USA*, **110**, 13660–13665.
- Zhao, J., Li, P., Motes, C.M., Park, S. and Hirschi, K.D. (2015) CHX14 is a plasma membrane K⁺-efflux transporter that regulates K⁺ redistribution in *Arabidopsis thaliana*. *Plant, Cell Environ.* **38**, 2223–2238.
- Zhou, R., Jackson, L., Shadle, G., Nakashima, J., Temple, S., Chen, F. and Dixon, R.A. (2010) Distinct cinnamoyl CoA reductases involved in parallel routes to lignin in *Medicago truncatula*. *Proc. Natl Acad. Sci. USA*, **107**, 17803–17808.
- Zhu, X.F., Lei, G.J., Wang, Z.W., Shi, Y.Z., Braam, J., Li, G.X. and Zheng, S.J. (2013) Coordination between apoplastic and symplastic detoxification confers plant aluminum resistance. *Plant Physiol.* **162**, 1947–1955.